

Capacity Limits of Full-Duplex Cellular Network

Kaiming Shen, *Student Member, IEEE*, Reza K. Farsani, *Student Member, IEEE*, and Wei Yu, *Fellow, IEEE*

Abstract—This paper explores the capacity limits of a wireless cellular network with full-duplex (FD) base station (BS) and half-duplex user terminals, in which three independent messages are communicated, i.e., uplink message m_1 from the uplink user to the BS, downlink message m_2 from the BS to the downlink user, and D2D message m_3 from the uplink user to the downlink user. Information theoretically, this wireless system can be interpreted as a generalization of the FD relay broadcast channel with side message transmitted from relay to destination. Our study starts with a simpler case that has only the uplink and the downlink transmissions of (m_1, m_2) . For the discrete memoryless channel model, we propose a novel strategy that uses the BS as a FD relay to facilitate interference cancellation. The paper further provides a new converse which is strictly tighter than the cut-set bound. Taken together and specialized to the Gaussian case, our inner and outer bounds yield a characterization of the capacity to within a constant gap for the scalar and the vector Gaussian channel models. Furthermore, the paper studies a general setup with (m_1, m_2, m_3) . For the discrete memoryless channel model, we incorporate Marton's broadcast coding to obtain an achievable rate region, which is larger than the existing ones. Regarding the converse, we derive a nontrivial outer bound by means of genie. For the scalar Gaussian channel model, it is shown that by using one of the two rate-splitting schemes depending on the channel condition, we can already achieve the capacity to within a constant gap. For the vector Gaussian channel model, we further show how dirty paper coding can be applied to coordinate the transmissions of (m_1, m_2, m_3) in three different ways. Finally, simulations demonstrate the advantages of using the BS as a relay in the FD cellular network.

Index Terms—Full-duplex cellular network, D2D transmission, relay broadcast channel with side message, approximate capacity.

I. INTRODUCTION

TRADITIONAL wireless cellular systems separate uplink and downlink signals by using either time division duplex (TDD) or frequency division duplex (FDD)—because at a conventional analog front-end, the echo due to transmitting in one direction can overwhelm the receiver in the other direction. However, recent progress in analog and digital echo cancellation [1]–[3] has opened up the possibility of realizing bi-directional communication in a full-duplex (FD) mode.

This paper considers an FD cellular network, in which the base station (BS) is capable of transmitting and receiving signals in the FD mode [4], but the uplink and downlink user terminals still operate in half-duplex mode. In such a system

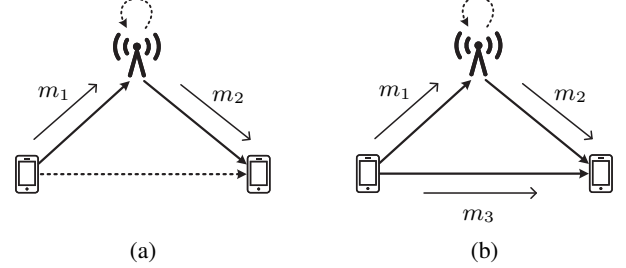


Fig. 1. (a) Full-duplex cellular network with only the uplink message m_1 and downlink message m_2 ; (b) Full-duplex cellular network with the D2D message m_3 included. The loops represent self-interference and the dashed link in (a) represents the uplink-to-downlink interference.

as depicted in Fig. 1(a), although the uplink transmission of m_1 and the downlink transmission of m_2 occupy the same spectrum band simultaneously thereby doubling the frequency-reuse factor as compared to TDD or FDD, the cross-channel interference from the uplink user (node 1) to the downlink user (node 3) would present as a major source of impairment. It is in fact the overall performance bottleneck as pointed out in [5], [6], especially when the uplink and downlink user terminals are in close proximity to each other. This paper aims to show that the resulting cross-channel interference can potentially be cancelled or significantly suppressed *with the aid from the BS*—the BS can act as a relay, as it already needs to decode the uplink message m_1 , therefore can help the downlink user cancel cross-channel interference due to m_1 . For the channel model with only (m_1, m_2) , this work improves the cut-set bound and proves that the rate region achieved by the proposed scheme is within a constant gap to the capacity region for the scalar Gaussian channel model as well as the vector Gaussian channel model in which the BS and the user terminals are equipped with multiple antennas.

In addition to the uplink and downlink transmissions, this paper further considers a channel model in which the uplink user wishes to directly send a separate message to the downlink user via the device-to-device (D2D) link. This new setup of the FD cellular network with D2D message m_3 , as shown in Fig. 6(b), is a generalization of the FD uplink-downlink cellular network in Fig. 6(a) with an extra D2D transmission. For this channel model, we propose incorporating Marton's broadcast coding [7] into the previous transmitting scheme with only (m_1, m_2) . We further introduce two rate-splitting schemes that are easier to implement, and propose a novel converse. In light of these inner and outer bounds, we show that using one of the two rate-splitting schemes (depending on the channel condition) suffices to attain the capacity to within a constant gap for the scalar Gaussian cellular network with D2D.

We point out that the FD cellular network with D2D is

Manuscript submitted December 15, 2024. This work is supported in part by Natural Sciences and Engineering Research Council (NSERC) of Canada and in part by Huawei Technologies Canada. The materials in this paper have been presented in part in IEEE Information Theory Workshop (ITW), December 2018, Guangzhou, China and in part in IEEE International Symposium on Information Theory (ISIT), July 2019, Paris, France. The authors are with The Edward S. Rogers Sr. Department of Electrical and Computer Engineering, University of Toronto, Toronto, ON M5S 3G4, Canada (e-mails: {kshen, rkfarsani, weiyu}@ece.utoronto.ca).

TABLE I
MAIN THEOREMS AND PROPOSITIONS OF THE PAPER

	Achievability	Converse	Approximate Capacity Region
Discrete Memoryless Channel without D2D	Theorem 1	Theorem 2	–
Scalar Gaussian Channel without D2D	Proposition 1	Proposition 3	Propositions 2 & 4; Theorem 3
Vector Gaussian Channel without D2D	Proposition 5	Proposition 6	Theorem 4
Discrete Memoryless Channel with D2D	Theorem 5	Theorem 6	–
Scalar Gaussian Channel with D2D	Propositions 9 & 10	Proposition 8	Theorem 7
Vector Gaussian Channel with D2D	Propositions 11, 12 & 13	Proposition 14	–

equivalent to the relay broadcast channel with side message (or with “private” message [8]). The authors of [8] propose a decode-and-forward scheme and a compress-and-forward scheme for this channel. Our scheme is a further development of the decode-and-forward scheme [8] by incorporating multiple new techniques (such as rate splitting, joint decoding, and Marton’s broadcast coding [7]). With respect to the converse, [8] derives an outer bound based on the genie-aided method, but as indicated by the authors, the outer bound of [8] is not computable. This paper develops better use of the auxiliary “genie” variables to improve upon the cut-set bound, and further comes up with a new sum-rate upper bound that would play a key role in characterizing the capacity region for the Gaussian case to within a constant gap.

The FD cellular network with D2D is also a generalization of the *partially-cooperative relay broadcast channel* [9], [10] for which a modified Marton’s broadcast coding scheme has already been proposed. The achievability part of our paper can be thought of as a generalization of [9], [10] in incorporating the transmission of the relay-to-destination message m_2 into the modified Marton’s coding. More importantly, the present paper is the first work to determine the capacity of the relay broadcast channel (with side message) to within a constant gap for a general scalar Gaussian channel setup.

For the conventional FD cellular network setup with only uplink and downlink transmissions and no D2D transmission, many earlier works [11]–[16] aim to alleviate the cross-channel interference by optimizing resource allocation. Unlike these optimization-based studies, the present work explores the fundamental limits. In particular, the paper characterizes the capacity region to within a constant gap for a Gaussian FD cellular network in general, as opposed to the existing works [17]–[19] that only consider the sum rates in the asymptotic regime. Furthermore, our capacity analyses are extended to the D2D case.

For ease of reference, we outline the principal theorems and propositions in Table I as displayed at the top of the page. What follows is a list of the main contributions classified by the channel models:

- *Discrete memoryless channel without D2D*: We propose new techniques to enhance the prior achievability and converse.
- *Scalar Gaussian channel without D2D*: We determine the capacity in the very strong interference regime. We also characterize the capacity to within 1 bit/s/Hz in general,

and to within 0.6358 bits/s/Hz in the strong interference regime.

- *Vector Gaussian channel without D2D*: We characterize the capacity region to within a constant gap when the BS and user terminals have multiple antennas.
- *Discrete memoryless channel with D2D*: We extend the achievability by incorporating Marton’s broadcast coding, and extend the converse by using a genie.
- *Scalar Gaussian channel with D2D*: We show that the capacity can already be attained to within 1 bit/s/Hz by using one of the two rate-splitting schemes depending on the channel condition; this constant-gap optimality carries over to the relay broadcast channel [9], [10].
- *Vector Gaussian channel with D2D*: We propose three different achievabilities based on dirty paper coding; we also provide a new converse tighter than the cut-set bound.

Throughout the paper, we use $[1 : N]$ to denote the set $\{1, 2, \dots, N\}$, $C(x)$ the function $\log_2(1 + x)$ for $x \geq 0$, \mathbb{C} the set of complex numbers, $\mathbb{S}_+^{n \times n}$ the set of $n \times n$ positive semidefinite matrices, \mathbf{I} the identity matrix, $(\cdot)^H$ the Hermitian transpose, $\text{Tr}(\cdot)$ the trace of matrix. We use a superscripted bold letter to denote a sequence of variables, e.g., $\mathbf{X}^N = (X_1, X_2, \dots, X_N)$, and further use $\mathbf{X}_{n_1}^{n_2}$ (with $n_2 > n_1$) to denote the subsequence $(X_{n_1}, X_{n_1+1}, \dots, X_{n_2})$. For a random variable X , we use $\mathbb{E}(X)$ to denote its expected value, and use $\text{Var}(X)$ to denote its variance. For two random variables X_1 and X_2 , we use $X_1 \perp\!\!\!\perp X_2$ to denote the independence, and use $\text{Cov}(X_1, X_2)$ to denote their covariance.

The rest of the paper is organized as follows. Section II introduces the different channel models of FD cellular network, i.e., the discrete memoryless channel, the scalar Gaussian channel, and the vector Gaussian channel, with or without D2D. Section III focuses on the no D2D case with uplink and downlink transmissions alone. Section IV looks into a more general setup with D2D link included. Section V presents simulation results. Finally, conclusion is drawn in Section VI.

II. SYSTEM MODEL

The FD cellular network models can be categorized according to the channel model (i.e., discrete memoryless channel, scalar Gaussian channel, or vector Gaussian channel) and the network topology (i.e., with or without D2D link). A total of six models are specified below.

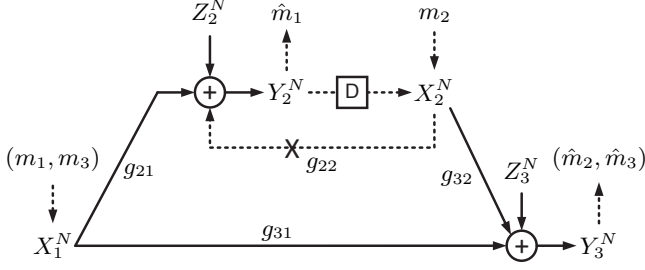


Fig. 2. Gaussian full-duplex relay broadcast channel with side message m_2 . Here, the block “D” refers to a one-epoch delay.

A. Without D2D Case

1) *Discrete Memoryless Channel*: We start with the discrete memoryless channel without D2D link as shown in Fig. 1(a). Let $X_{in} \in \mathcal{X}_i$ be the transmitted signal of node $i \in \{1, 2\}$ and $Y_{jn} \in \mathcal{Y}_j$ be the received signal at node $j \in \{2, 3\}$, at the n th channel use, over the alphabet sets $(\mathcal{X}_1, \mathcal{X}_2, \mathcal{Y}_2, \mathcal{Y}_3)$. The discrete memoryless channel is defined by the channel transition probability $p(y_{2n}, y_{3n} | x_{1n}, x_{2n})$. Over a total of N channel uses, node 1 wishes to send $m_1 \in [1 : 2^{NR_1}]$ to node 2, while node 2 wishes to send $m_2 \in [1 : 2^{NR_2}]$ to node 3, where R_1 and R_2 are referred to as the uplink rate and the downlink rate, respectively. The encoding of X_{1n} solely depends on m . In comparison, since the transmitter of X_{2n} and the receiver of Y_{2n} are co-located at node 2, the encoding of X_{2n} can depend on the past received signals \mathbf{Y}_2^{n-1} :

$$X_{1n} = \mathcal{E}_1(m_1, n) \text{ and } X_{2n} = \mathcal{E}_2(m_2, \mathbf{Y}_2^{n-1}, n), \quad (1)$$

for $n \in [1 : N]$. After N channel uses, node 3 decodes m_2 based on \mathbf{Y}_3^N . Because node 2 itself is the downlink transmitter, it can make use of \mathbf{X}_2^N in addition to \mathbf{Y}_2^N in decoding m_1 , i.e.,

$$\hat{m}_1 = \mathcal{D}_1(\mathbf{Y}_2^N, \mathbf{X}_2^N) \text{ and } \hat{m}_2 = \mathcal{D}_2(\mathbf{Y}_3^N). \quad (2)$$

An uplink-and-downlink rate pair (R_1, R_2) is said to be achievable if there exists a set of deterministic functions $(\mathcal{E}_1, \mathcal{E}_2, \mathcal{D}_2, \mathcal{D}_3)$ such that the probability of error, $\Pr\{(\hat{m}_1, \hat{m}_2) \neq (m_1, m_2)\}$, tends to zero as $N \rightarrow \infty$.

2) *Scalar Gaussian Channel*: The above discrete memoryless channel model can be specialized to the vector Gaussian case by letting $X_{in}, Y_{jn} \in \mathbb{C}$, and by imposing power constraints on X_{in} , i.e., $\sum_{n=1}^N |X_{in}|^2 \leq NP_i$. As illustrated in Fig. 2, we have

$$Y_{2n} = g_{21}X_{1n} + Z_{2n}, \quad (3)$$

$$Y_{3n} = g_{31}X_{1n} + g_{32}X_{2n} + Z_{3n}, \quad (4)$$

for $n \in [1 : N]$, where $g_{ji} \in \mathbb{C}$ is the channel gain from the transmitter node i to the receiver node j , and $Z_{jn} \sim \mathcal{CN}(0, \sigma^2)$ for the fixed $\sigma^2 > 0$ is the additive white Gaussian noise at node j in the n th channel use. Due to the fact that the BS (i.e., node 2) operates in a full-duplex mode, the self-interference at the relay has been removed implicitly, as illustrated in Fig. 2.

3) *Vector Gaussian Channel*: Assuming that node i has L_i^+ transmit antennas and L_i^- receive antennas, we can extend the

above scalar Gaussian channel to the multi-antenna case:

$$\mathbf{Y}_{2n} = \mathbf{G}_{21}\mathbf{X}_{1n} + \mathbf{Z}_{2n}, \quad (5)$$

$$\mathbf{Y}_{3n} = \mathbf{G}_{31}\mathbf{X}_{1n} + \mathbf{G}_{32}\mathbf{X}_{2n} + \mathbf{Z}_{3n}, \quad (6)$$

where $\mathbf{Y}_{jn} \in \mathbb{C}^{L_j^-}$, $\mathbf{X}_{in} \in \mathbb{C}^{L_i^+}$, $\mathbf{G}_{ji} \in \mathbb{C}^{L_j^- \times L_i^+}$, and $\mathbf{Z}_j \in \mathbb{C}^{L_j^-}$ are the multidimensional versions of Y_{jn} , X_{in} , g_{ji} , and Z_{jn} , respectively. In this case, the power constraint becomes $\sum_{n=1}^N \text{Tr}(\mathbf{X}_{in}\mathbf{X}_{in}^H) \leq NP_i$, and the additive white Gaussian noise becomes $\mathbf{Z}_{jn} \sim \mathcal{CN}(\mathbf{0}, \sigma^2 \mathbf{I})$.

B. D2D Case

For the D2D case as shown in Fig. 1(b), we focus on the discrete memoryless channel since it can be specialized to the scalar Gaussian channel and the vector Gaussian channel as in the previous section. We now include a direct transmission of $m_3 \in [1 : 2^{NR_3}]$ from node 1 to node 3 in the discrete memoryless channel model as described in Section II-A; R_3 is referred to as the D2D rate. The channel setup, i.e., the alphabet sets $(\mathcal{X}_1, \mathcal{X}_2, \mathcal{Y}_2, \mathcal{Y}_3)$ and the channel transition probability $p(y_{2n}, y_{3n} | x_{1n}, x_{2n})$, remains the same as before. Because m_1 and m_3 are both transmitted from node 1, the encoding of X_1 now depends on (m_1, m_3) , i.e.,

$$X_{1n} = \mathcal{E}_1(m_1, m_3, n) \text{ and } X_{2n} = \mathcal{E}_2(m_2, \mathbf{Y}_2^{n-1}, n). \quad (7)$$

Moreover, since m_2 and m_3 are both intended for node 3, we define the decoding functions differently:

$$\hat{m}_1 = \mathcal{D}_1(\mathbf{Y}_2^N, \mathbf{X}_2^N) \text{ and } (\hat{m}_2, \hat{m}_3) = \mathcal{D}_2(\mathbf{Y}_3^N). \quad (8)$$

Similarly, a rate triple (R_1, R_2, R_3) is said to be achievable if there exists a set of deterministic functions $(\mathcal{E}_1, \mathcal{E}_2, \mathcal{D}_1, \mathcal{D}_2)$ such that the probability of error, $\Pr\{(\hat{m}_1, \hat{m}_2, \hat{m}_3) \neq (m_1, m_2, m_3)\}$, tends to zero as $N \rightarrow \infty$.

III. CAPACITY LIMITS OF FD CELLULAR NETWORK WITHOUT D2D

This section examines the FD cellular network with an uplink and a downlink message only. We start with the discrete memoryless channel model then treat the scalar/vector Gaussian channel model.

A. Achievability for Discrete Memoryless Channel without D2D

As mentioned earlier, the cross-channel interference from node 1 to node 3 is the main bottleneck [4]. To address this issue, we use the BS (i.e., node 2) as a relay to facilitate cancelling the interfering signal at node 3. We further propose to split message m_1 (which causes the interference) so that node 3 can at least cancel a portion of the interference. The resulting achievable rate region is stated below.

Theorem 1: For the discrete memoryless channel, a rate pair (R_1, R_2) is achievable if it is in the convex hull of

$$R_1 \leq I(X_1; Y_2 | U, X_2), \quad (9a)$$

$$R_2 \leq I(X_2; Y_3 | U, V), \quad (9b)$$

$$R_1 + R_2 \leq I(X_1; Y_2 | U, V, X_2) + I(U, V, X_2; Y_3), \quad (9c)$$

TABLE II
PROPOSED CODING SCHEME FOR THE NO D2D CASE.

t	1	2	\dots	$T-1$	T
X_1	$\mathbf{x}_1^N(m_{11}^1 m_{10}^1, 1)$	$\mathbf{x}_1^N(m_{11}^2 m_{10}^2, m_{10}^1)$	\rightarrow	$\mathbf{x}_1^N(m_{11}^{T-1} m_{10}^{T-1}, m_{10}^{T-2})$	$\mathbf{x}_1^N(1 1, m_{10}^{T-1})$
Y_2	$(\hat{m}_{10}^1, \hat{m}_{11}^1)$	$(\hat{m}_{10}^2, \hat{m}_{11}^2)$	\rightarrow	$(\hat{m}_{10}^{T-1}, \hat{m}_{11}^{T-1})$	\emptyset
X_2	$\mathbf{x}_2^N(m_2^1 1)$	$\mathbf{x}_2^N(m_2^2 \hat{m}_{10}^1)$	\rightarrow	$\mathbf{x}_2^N(m_2^{T-1} \hat{m}_{10}^{T-2})$	$\mathbf{x}_2^N(m_2^T \hat{m}_{10}^{T-1})$
Y_3	$(1, \hat{m}_2^1)$	$(\hat{m}_{10}^1, \hat{m}_2^2)$	\leftarrow	$(\hat{m}_{10}^{T-2}, \hat{m}_2^{T-1})$	$(\hat{m}_{10}^{T-1}, \hat{m}_2^T)$

for some $p(u)p(v, x_1|u)p(x_2|u)$.

Proof: Split m_1 into a common-private message pair $(m_{10}, m_{11}) \in [1 : 2^{NR_{10}}] \times [1 : 2^{NR_{11}}]$ with $R_{10} + R_{11} = R_1$; the common message m_{10} is aimed at both receivers (i.e., node 2 and node 3), while the private message m_{11} is aimed at the intended receiver (i.e., node 2). Introduce a total of T blocks for the block-Markov coding. For each block $t \in [1 : T]$, in an independent and identically distributed (i.i.d.) manner according to their respective distributions as in $p(u)p(v, x_1|u)p(x_2|u)$, generate the following codebooks:

- Relay codebook $\mathbf{u}^N(m_{10}^{t-1})$;
- Uplink common codebook $\mathbf{v}^N(m_{10}^t|m_{10}^{t-1})$;
- Uplink private codebook $\mathbf{x}_1^N(m_{11}^t|m_{10}^t, m_{10}^{t-1})$;
- Downlink codebook $\mathbf{x}_2^N(m_2^t|m_{10}^{t-1})$.

In block t , knowing its past common message m_{10}^{t-1} , node 1 transmits $\mathbf{x}_1^N(m_{11}^t|m_{10}^t, m_{10}^{t-1})$; we set $m_{10}^0 = m_{10}^T = m_{11}^T = 0$ by default.

In block t , after obtaining \hat{m}_{10}^{t-1} from the previous block $t-1$, node 2 transmits $\mathbf{x}_2^N(m_2^t|\hat{m}_{10}^{t-1})$, and recovers $(\hat{m}_{10}^t, \hat{m}_{11}^t)$ jointly (e.g., by the joint typicality) from the received signal \mathbf{y}_2^N ; $\Pr\{(\hat{m}_{10}^t, \hat{m}_{11}^t) \neq (m_{10}^t, m_{11}^t)\}$ tends to zero as $N \rightarrow \infty$ provided that

$$R_{11} \leq I(X_1; Y_2|U, V, X_2), \quad (10)$$

$$R_{10} + R_{11} \leq I(X_1; Y_2|U, X_2). \quad (11)$$

Node 3 decodes the blocks in a *backward* direction, i.e., block $t-1$ prior to block t . In block t , after obtaining \hat{m}_{10}^t from the previous block $t+1$, node 3 recovers $(\hat{m}_{10}^{t-1}, \hat{m}_2^t)$ jointly from the received signal \mathbf{y}_3^N ; $\Pr\{(\hat{m}_{10}^{t-1}, \hat{m}_2^t) \neq (m_{10}^{t-1}, m_2^t)|\hat{m}_{10}^{t-1} = m_{10}^{t-1}\}$ tends to zero as $N \rightarrow \infty$ if

$$R_2 \leq I(X_2; Y_3|U, V), \quad (12)$$

$$R_{10} + R_2 \leq I(U, V, X_2; Y_3). \quad (13)$$

The overall error probability P_e , namely $\Pr((\hat{m}_1, \hat{m}_2) \neq (m_1, m_2))$ can be upper bounded as

$$P_e \leq \frac{1}{T} \cdot \sum_{t=1}^T \left[\Pr\{(\hat{m}_{10}^t, \hat{m}_{11}^t) \neq (m_{10}^t, m_{11}^t)\} + \Pr\{(\hat{m}_{10}^{t-1}, \hat{m}_2^t) \neq (m_{10}^{t-1}, m_2^t)|\hat{m}_{10}^{t-1} = m_{10}^{t-1}\} \right], \quad (14)$$

so P_e tends to zero as $N \rightarrow \infty$ if (10)–(13) are satisfied. Furthermore, combining (10)–(13) with $R_{10}, R_{11} \geq 0$ and $R_1 = R_{10} + R_{11}$ by using the Fourier-Motzkin elimination, we obtain the inner bound in (9). Note that the effective uplink rate equals to $(T-1)/T \cdot R_1$, since block T with $m_{10}^T = m_{11}^T = 0$

is not used for transmitting m_1 . The achievability of (9) is established by letting $T \rightarrow \infty$. ■

Table II illustrates the encoding-and-decoding procedure as stated in the above proof; the arrows indicate in which order the blocks are processed.

In Theorem 1, it can be seen that the auxiliary variable U is the enabler of the relaying at node 2, which aims to assist node 3 in canceling the cross-channel interference. The resulting achievable rate region is in general larger than that of the no relaying scheme (with $U = \emptyset$).

B. Converse for Discrete Memoryless Channel without D2D

The authors of [8] propose an outer bound on (R_1, R_2, R_3) for a more general model with D2D. When specialized to the no D2D case, i.e., when $R_3 = 0$, their converse amounts to the cut-set bound which consists of two individual upper bounds on R_1 or R_2 . The contribution of this section is to propose a new upper bound on $R_1 + R_2$ that improves the cut-set bound. As shown later in Sections III-C and III-D, this new upper bound plays a key role in characterizing the capacity region to within a constant gap for the Gaussian case. Our converse is specified in the theorem below.

Theorem 2: For the discrete memoryless channel, any achievable rate pair (R_1, R_2) must be in the convex hull of

$$R_1 \leq I(X_1; Y_2|X_2), \quad (15a)$$

$$R_2 \leq I(X_2; Y_3|X_1), \quad (15b)$$

$$R_1 + R_2 \leq I(X_1; Y_2, Y_3|X_2) + I(X_2; Y_3), \quad (15c)$$

for some $p(x_1, x_2)$.

Proof: Observe that (15a) and (15b) are directly from the cut-set bound. Regarding $R_1 + R_2$, we have

$$\begin{aligned} & N(R_1 + R_2 - \epsilon_N) \\ & \leq I(M_1; \mathbf{Y}_2^N, \mathbf{X}_2^N) + I(M_2; \mathbf{Y}_3^N) \\ & \stackrel{(a)}{\leq} I(M_1; \mathbf{Y}_2^N, \mathbf{X}_2^N, \mathbf{Y}_3^N|M_2) + I(M_2; \mathbf{Y}_3^N) \\ & \stackrel{(b)}{=} I(M_1; \mathbf{Y}_2^N, \mathbf{Y}_3^N|M_2) + I(M_2; \mathbf{Y}_3^N) \\ & \leq \sum_{n=1}^N \left[I(M_1; Y_{2n}, Y_{3n}|M_2, \mathbf{Y}_2^{n-1}, \mathbf{Y}_3^{n-1}) \right. \\ & \quad \left. + I(M_2, \mathbf{Y}_2^{n-1}, \mathbf{Y}_3^{n-1}; Y_{3n}) \right] \\ & \stackrel{(c)}{=} \sum_{n=1}^N \left[I(M_1; Y_{2n}, Y_{3n}|M_2, \mathbf{Y}_2^{n-1}, \mathbf{Y}_3^{n-1}, X_{2n}) \right. \\ & \quad \left. + I(M_2, \mathbf{Y}_2^{n-1}, \mathbf{Y}_3^{n-1}, X_{2n}; Y_{3n}) \right] \end{aligned}$$

$$\begin{aligned}
&\leq \sum_{n=1}^N \left[I(M_1, M_2, \mathbf{Y}_2^{n-1}, \mathbf{Y}_3^{n-1}; Y_{2n}, Y_{3n} | X_{2n}) \right. \\
&\quad \left. + I(X_{2n}; Y_{3n}) \right] \\
&\stackrel{(d)}{=} \sum_{n=1}^N \left[I(X_{1n}; Y_{2n}, Y_{3n} | X_{2n}) + I(X_{2n}; Y_{3n}) \right] \\
&\leq NI(X_1; Y_2, Y_3 | X_2) + NI(X_2; Y_3), \tag{16}
\end{aligned}$$

where ϵ_N tends to zero as $N \rightarrow \infty$ by Fano's inequality, (a) follows as $M_1 \perp\!\!\!\perp M_2$, (b) and (c) both follow as X_{2n} is a function of $(M_2, \mathbf{Y}_2^{n-1})$, (d) follows as $(M_1, M_2, \mathbf{Y}_2^{n-1}, \mathbf{Y}_3^{n-1}) \rightarrow X_{1n} \rightarrow (Y_{2n}, Y_{3n})$ form a Markov chain conditioned on X_{2n} . The converse is then verified. ■

C. Scalar Gaussian Channel without D2D

We now characterize the capacity region of the scalar Gaussian channel to within one bit.

First, we consider the achievability. Although the achievable rate region as stated in the following proposition can be obtained by evaluating the mutual information bounds of Theorem 1 directly, we present a proof based on a *binning* scheme at the relay.

Proposition 1: For the scalar Gaussian channel, a rate pair (R_1, R_2) is achievable if it is in the convex hull of

$$R_1 \leq \mathcal{C}\left(\frac{(b+c)|g_{21}|^2 P_1}{\sigma^2}\right), \tag{17a}$$

$$R_2 \leq \mathcal{C}\left(\frac{e|g_{32}|^2 P_2}{\sigma^2 + c|g_{31}|^2 P_1}\right), \tag{17b}$$

$$\begin{aligned}
R_1 + R_2 \leq &\mathcal{C}\left(\frac{(a+b)|g_{31}|^2 P_1 + |g_{32}|^2 P_2 + J\sqrt{ad}}{\sigma^2 + c|g_{31}|^2 P_1}\right) \\
&+ \mathcal{C}\left(\frac{c|g_{21}|^2 P_1}{\sigma^2}\right), \tag{17c}
\end{aligned}$$

for some parameters $a, b, c, d, e \geq 0$ with $a + b + c \leq 1$ and $d + e \leq 1$, where

$$J = 2|g_{31}g_{32}|\sqrt{P_1 P_2}. \tag{18}$$

Proof: The main idea is still to let node 2 help interference cancellation at node 3, but through the bin index. As before, split m_1 into a common-private message pair $(m_{10}, m_{11}) \in [1 : 2^{NR_{10}}] \times [1 : 2^{NR_{11}}]$, where $R_{10} + R_{11} = R_1$. Furthermore, randomly partition the set of m_{10} into 2^{NR_B} equal-size bins (with $R_B \leq R_{10}$). We use the function $\ell = \mathcal{B}(m_{10})$ to denote the bin index ℓ of each m_{10} . A block Markov procedure is performed across T blocks. The codebooks are generated independently according to i.i.d. Gaussian distribution $\mathcal{CN}(0, 1)$:

- Binning codebook $\mathbf{u}^N(\ell^{t-1})$;
- Uplink common codebook $\tilde{\mathbf{v}}^N(m_{10}^t)$;
- Uplink private codebook $\mathbf{w}_1^N(m_{11}^t)$;
- Downlink codebook $\mathbf{w}_2^N(m_2^t)$.

We remark that the uplink common codebook here is denoted by $\tilde{\mathbf{v}}^N$ rather than \mathbf{v}^N in order to highlight its difference from the auxiliary variable V of (9). In contrast to V that reflects the

encoding of m_{10} conditioned on some past message, $\tilde{\mathbf{v}}^N$ only captures the current message m_{10} . For ease of interpretation, we further introduce a codebook corresponding to V in (9):

$$\mathbf{v}^N(m_{10}^t | \ell^{t-1}) = \sqrt{aP_1} \mathbf{u}^N(\ell^{t-1}) + \sqrt{bP_1} \tilde{\mathbf{v}}^N(m_{10}^t). \tag{19}$$

In block t , with the bin index $\ell^{t-1} = \mathcal{B}(m_{10}^{t-1})$, node 1 transmits

$$\mathbf{x}_1^N(t) = \mathbf{v}^N(m_{10}^t | \ell^{t-1}) + \sqrt{cP_1} \mathbf{w}_1^N(m_{11}^t). \tag{20}$$

In block t , after obtaining $\hat{\ell}_{10}^{t-1}$ from the previous block $t-1$, node 2 transmits

$$\mathbf{x}_2^N = \sqrt{dP_2} \mathbf{u}^N(\hat{\ell}_{10}^{t-1}) + \sqrt{eP_2} \mathbf{w}_2^N(m_2^t), \tag{21}$$

and subtracts $\sqrt{aP_1} \mathbf{u}^N(\ell^{t-1})$ from its received signal \mathbf{y}_2^N , then recovers \hat{m}_{10}^t and \hat{m}_{11}^t via successive cancellation, which is successful if

$$R_{10} \leq I(V; Y_2 | U, X_2) = \mathcal{C}\left(\frac{b|g_{21}|^2 P_1}{\sigma^2 + c|g_{21}|^2 P_1}\right), \tag{22}$$

$$R_{11} \leq I(X_1; Y_2 | U, V, X_2) = \mathcal{C}\left(\frac{c|g_{21}|^2 P_1}{\sigma^2}\right). \tag{23}$$

After decoding in block t , node 2 computes $\hat{\ell}^t = \mathcal{B}(\hat{m}_{10}^t)$ which is used in the next block $t+1$.

Node 3 decodes the blocks in a backward direction. In block t , it first recovers the binning index $\hat{\ell}^{t-1}$ cooperatively transmitted by X_1 and X_2 at rate

$$\begin{aligned}
R_B &\leq I(U; Y_3) \\
&= \mathcal{C}\left(\frac{(|g_{31}|\sqrt{aP_1} + |g_{32}|\sqrt{dP_2})^2}{\sigma^2 + (b+c)|g_{31}|^2 P_1 + e|g_{32}|^2 P_2}\right), \tag{24}
\end{aligned}$$

which guarantees that the error probability $\Pr\{\hat{\ell}^{t-1} \neq \ell^{t-1} | \hat{\ell}^{t-1} = \ell^{t-1}\}$ tends to zero as $N \rightarrow \infty$; $\mathbf{u}^N(\hat{\ell}^{t-1})$ is then subtracted from \mathbf{y}^N . Furthermore, in block t , with $\hat{\ell}^t$ obtained from the previous block $t+1$, node 3 finds a pair of $(\hat{m}_{10}^t, \hat{m}_2^t)$ according to the joint typicality under the constraint that

$$\mathcal{B}(\hat{m}_{10}^t) = \hat{\ell}^t. \tag{25}$$

This joint decoding is successful if

$$R_2 \leq I(X_2; Y_3 | U, V) = \mathcal{C}\left(\frac{e|g_{32}|^2 P_2}{\sigma^2 + c|g_{31}|^2 P_1}\right), \tag{26}$$

and

$$\begin{aligned}
R_2 + (R_{10} - R_B) &\leq I(V, X_2; Y_3 | U) \\
&= \mathcal{C}\left(\frac{e|g_{32}|^2 P_2 + b|g_{31}|^2 P_1}{\sigma^2 + c|g_{31}|^2 P_1}\right). \tag{27}
\end{aligned}$$

The inequalities (22), (23), (24), (26), and (27), along with $R_B \leq R_{10}$, $R_1 = R_{10} + R_{11}$ and $R_B, R_{10}, R_{11} \geq 0$, yield (17) as $T \rightarrow \infty$. ■

Remark 1: The main benefit of explicitly using binning in the above proof is that the binning scheme can be implemented via the incremental redundancy coding in practice, similar to its use in hybrid automatic repeat request (HARQ) [20] where the parity bits of the message are transmitted to help the eventual decoding.

Remark 2: We could have used successive cancellation and time sharing at node 3 to achieve the same inner bound as in Proposition 1, i.e., either recovering \hat{m}_{11}^t then \hat{m}_2^t or recovering \hat{m}_2^t then \hat{m}_{11}^t . In this case, to guarantee successful decoding, the condition

$$R_{10} - R_B \leq I(V; Y_3 | U, X_2) = C \left(\frac{b|g_{31}|^2 P_1}{\sigma^2 + c|g_{31}|^2 P_1} \right) \quad (28)$$

is required in addition to (26) and (27). It can be proved however that this additional constraint does not reduce the achievable rate region.

However, the relaying at node 2 is sometimes not useful, as stated in the following proposition.

Proposition 2: For the scalar Gaussian FD cellular network, in the *very strong interference* regime such that $|g_{31}|^2 \geq |g_{21}|^2(1 + |g_{32}|^2)$, the capacity region of the rate pair (R_1, R_2) is

$$R_1 \leq C \left(\frac{|g_{21}|^2 P_1}{\sigma^2} \right), \quad (29a)$$

$$R_2 \leq C \left(\frac{|g_{32}|^2 P_2}{\sigma^2} \right). \quad (29b)$$

Proof: The achievability is verified directly by setting $a = c = d = 0$ and $b = e = 1$ in (17); note that the inner bound (17c) on $R_1 + R_2$ becomes redundant given $|g_{31}|^2 \geq |g_{21}|^2(1 + |g_{32}|^2)$. The converse follows from the cut-set bound. ■

Remark 3: The above capacity result cannot be carried over to the discrete memoryless case because the inner bound distribution $p(x_1)p(x_2)$ and the cut-set bound distribution $p(x_1, x_2)$ do not necessarily yield the same rate region of $R_1 \leq I(X_1; Y_2 | X_2)$ and $R_2 \leq I(X_2; Y_3 | X_1)$.

Next, we consider the converse. The following outer bound is directly from Theorem 2.

Proposition 3: For the scalar Gaussian channel, any achievable rate pair (R_1, R_2) must be in the convex hull of

$$R_1 \leq C \left(\frac{(1 - \rho^2)|g_{21}|^2 P_1}{\sigma^2} \right), \quad (30a)$$

$$R_2 \leq C \left(\frac{(1 - \rho^2)|g_{32}|^2 P_2}{\sigma^2} \right), \quad (30b)$$

$$R_1 + R_2 \leq C \left(\frac{|g_{31}|^2 P_1 + |g_{32}|^2 P_2 + J\rho}{\sigma^2} \right) + C \left(\frac{(1 - \rho^2)|g_{21}|^2 P_1}{\sigma^2 + (1 - \rho^2)|g_{31}|^2 P_1} \right), \quad (30c)$$

for some $\rho \in [0, 1]$, where J is defined in (18).

Proof: Let $\rho = \frac{1}{\sqrt{P_1 P_2}} \mathbb{E}(X_1 X_2)$; observe that $\rho \in [-1, 1]$. We first evaluate (15a):

$$\begin{aligned} R_1 &\leq I(X_1; Y_2 | X_2) \\ &= h(g_{21}X_1 + Z_2 | X_2) - h(Z_2) \\ &\leq \log \left(\frac{1}{\sigma^2} \text{Var}(g_{21}X_1 | X_2) \right) \\ &\stackrel{(a)}{\leq} C \left(\frac{1}{\sigma^2} \left(\mathbb{E}(|g_{21}X_1|^2) - \frac{\mathbb{E}^2(|g_{21}X_1 X_2|)}{\mathbb{E}(|X_2|^2)} \right) \right) \\ &= C \left(\frac{(1 - \rho^2)|g_{21}|^2 P_1}{\sigma^2} \right), \end{aligned} \quad (31)$$

where (a) follows as the general minimum mean squared error (MMSE) is upper bounded by the linear MMSE; (30b) can be obtained similarly. Moreover, with

$$\text{LMMSE} = \text{Var}(Y_2) - \text{Cov}(Y_2, [X_2, Y_3]) \cdot \text{Var}^{-1}([X_2, Y_3]) \cdot \text{Cov}^\dagger(Y_2, [X_2, Y_3]), \quad (32)$$

we can evaluate (15c) as follows:

$$\begin{aligned} R_1 + R_2 &\leq I(X_1; Y_2, Y_3 | X_2) + I(X_2; Y_3) \\ &= h(Y_2 | Y_3, X_2) - h(Z_2, Z_3) + h(Y_3) \\ &\leq \log \left(\frac{1}{\sigma^2} \text{Var}(Y_2 | Y_3, X_2) \right) + \log \left(\frac{1}{\sigma^2} \text{Var}(Y_3) \right) \\ &\stackrel{(b)}{\leq} \log \left(\frac{\text{LMMSE}}{\sigma^2} \right) + \log \left(\frac{1}{\sigma^2} \text{Var}(Y_3) \right) \\ &= C \left(\frac{(1 - \rho^2)|g_{21}|^2 P_1}{\sigma^2 + (1 - \rho^2)|g_{31}|^2 P_1} \right) + \\ &\quad C \left(\frac{|g_{31}|^2 P_1 + |g_{32}|^2 P_2 + J\rho}{\sigma^2} \right), \end{aligned} \quad (33)$$

where (b) follows by the aforementioned property of MMSE. Since further confining ρ to $[0, 1]$ does not reduce the rate region (30), the converse of this proposition is established. ■

Definition 1: An inner bound \mathcal{I} is said to be within a constant gap $\delta \geq 0$ to the capacity \mathcal{C} if $(R_1 + \delta, R_2 + \delta, \dots, R_k + \delta)$ is not inside \mathcal{C} for any $(R_1, R_2, \dots, R_k) \in \mathcal{I}$.

The main result of this section is stated below; we remark that the new outer bound (30c) on $R_1 + R_2$ is critical to proving a constant-gap optimality.

Theorem 3: For the scalar Gaussian channel, the inner bound of Proposition 1 is within 1 bit/s/Hz to the capacity region.

Proof: We use the power splitting strategy of [21] to set $a = 0$, $c = \min\{1, \sigma^2/(|g_{31}|^2 P_1)\}$, $b = 1 - c$, $d = 0$, and $e = 1$ in (17). Comparing the resulting inner bound to the outer bound (30) yields a constant gap of 1 bit/s/Hz. ■

Remark 4: The above proof with $a = d = 0$ implies that the rate-splitting scheme without relaying at node 2 already attains close to the capacity region. In other words, the gain of (R_1, R_2) reaped from using the BS as relay is limited by 1 bit. Nevertheless, as shown later in Section IV, relaying is crucial in enabling an achievability within a constant gap to the capacity region of the D2D case.

Remark 5: In proving this constant-gap optimality, the upper bound on $R_1 + R_2$ as newly introduced in this work plays a key role. In contrast, the cut-set bound used in [8] is not tight enough to approximate the capacity region.

We further show a case in which a judicious choice of (a, d) outperforms $a = d = 0$ in terms of the constant gap.

Proposition 4: For the scalar Gaussian channel, in the *strong interference* regime such that $|g_{31}| \geq |g_{21}|$, the achievable region of (R_1, R_2) as in Proposition 1 is within $\frac{1}{2} + \frac{1}{2} \log_2(\frac{\sqrt{2}+1}{2}) \approx 0.6358$ bits/s/Hz to the capacity region.

Proof: For each $\rho \in [0, 1]$ in (30), we correspondingly let $a = d = \rho^2$, $b = e = 1 - \rho^2$, and $c = 0$ in (17). Contrasting the resulting (17) with (30), we find that the gap is determined by the inner and outer bounds of $R_1 + R_2$, namely (17c) and (30c). Consequently, using the condition $|g_{31}| \geq |g_{21}|$, we obtain the following upper bound on the constant gap δ to the

capacity region:

$$\begin{aligned} 2\delta &\leq 1 + \mathcal{C}\left(\frac{|g_{31}|^2 P_1 + |g_{32}|^2 P_2 + J\rho}{\sigma^2}\right) \\ &\quad - \mathcal{C}\left(\frac{|g_{31}|^2 P_1 + |g_{32}|^2 P_2 + J\rho^2}{\sigma^2}\right) \\ &= 1 + \log_2\left(\frac{\lambda + \rho}{\lambda + \rho^2}\right), \end{aligned} \quad (34)$$

where

$$\lambda = \frac{|g_{31}|^2 P_1 + |g_{32}|^2 P_2 + \sigma^2}{J}. \quad (35)$$

By (18), it is clear that $\lambda \geq 1$. Thus, the solution to the following optimization problem is an upper bound on δ :

$$\text{maximize}_{\lambda, \rho} \quad \frac{\lambda + \rho}{\lambda + \rho^2} \quad (36a)$$

$$\text{subject to} \quad \lambda \geq 1, \quad (36b)$$

$$0 \leq \rho \leq 1. \quad (36c)$$

This problem is quasi-convex and thus can be optimally solved by the first-order condition, so $\lambda^* = 1$ and $\rho^* = \sqrt{2} - 1$. Substituting (λ^*, ρ^*) back in (34) verifies the theorem. ■

D. Vector Gaussian Channel without D2D

This section aims to extend the previous results to the multi-antenna case. Toward this end, we develop a multidimensional extension for the achievability and the converse.

We start with the achievability. The following proposition is an extension of Proposition 1.

Proposition 5: For the vector Gaussian channel, a rate pair (R_1, R_2) is achievable if it is in the convex hull of

$$R_1 \leq \log \left| \mathbf{I} + \frac{1}{\sigma^2} \mathbf{G}_{21} (\mathbf{K}_b + \mathbf{K}_c) \mathbf{G}_{21}^H \right|, \quad (37a)$$

$$R_2 \leq \log \frac{|\sigma^2 \mathbf{I} + \mathbf{G}_{31} \mathbf{K}_c \mathbf{G}_{31}^H + \mathbf{G}_{32} \mathbf{K}_e \mathbf{G}_{32}^H|}{|\sigma^2 \mathbf{I} + \mathbf{G}_{31} \mathbf{K}_c \mathbf{G}_{31}^H|}, \quad (37b)$$

$$\begin{aligned} R_1 + R_2 &\leq \log \frac{|\sigma^2 \mathbf{I} + \Phi|}{|\sigma^2 \mathbf{I} + \mathbf{G}_{31} \mathbf{K}_c \mathbf{G}_{31}^H|} + \\ &\quad \log \left| \mathbf{I} + \frac{1}{\sigma^2} (\mathbf{G}_{21} \mathbf{K}_c \mathbf{G}_{21}^H) \right|, \end{aligned} \quad (37c)$$

for some parameters $\mathbf{\Lambda}_a \in \mathbb{C}^{L_1^+ \times \min\{L_1^+, L_2^+\}}$, $\mathbf{\Lambda}_b \in \mathbb{C}^{L_1^+ \times L_1^+}$, $\mathbf{\Lambda}_c \in \mathbb{C}^{L_1^+ \times L_1^+}$, $\mathbf{\Lambda}_d \in \mathbb{C}^{L_2^+ \times \min\{L_1^+, L_2^+\}}$, $\mathbf{\Lambda}_e \in \mathbb{C}^{L_2^+ \times L_2^+}$ with $\text{Tr}(\mathbf{K}_a + \mathbf{K}_b + \mathbf{K}_c) \leq P_1$ and $\text{Tr}(\mathbf{K}_d + \mathbf{K}_e) \leq P_2$, where $\mathbf{K}_i = \mathbf{\Lambda}_i \mathbf{\Lambda}_i^H$, $\forall i \in \{a, b, c, d, e\}$, and

$$\begin{aligned} \Phi &= \mathbf{G}_{31} (\mathbf{K}_a + \mathbf{K}_b + \mathbf{K}_c) \mathbf{G}_{31}^H + \mathbf{G}_{32} (\mathbf{K}_d + \mathbf{K}_e) \mathbf{G}_{32}^H \\ &\quad + \mathbf{G}_{31} \mathbf{\Lambda}_a \mathbf{\Lambda}_a^H \mathbf{G}_{31}^H + \mathbf{G}_{32} \mathbf{\Lambda}_d \mathbf{\Lambda}_d^H \mathbf{G}_{32}^H. \end{aligned} \quad (38)$$

Proof: The coding scheme here follows that of Proposition 1 closely, so we only highlight their difference. The following codebooks are generated independently according to the i.i.d. Gaussian distribution $\mathcal{CN}(0, 1)$:

- Binning codebook $\mathbf{U}^N(\ell^{t-1}) \in \mathbb{C}^{\min\{L_1^+, L_2^+\} \times N}$;
- Uplink common codebook $\tilde{\mathbf{V}}^N(m_{10}^t) \in \mathbb{C}^{L_1^+ \times N}$;
- Uplink private codebook $\mathbf{W}_1^N(m_{11}^t) \in \mathbb{C}^{L_1^+ \times N}$;
- Downlink codebook $\mathbf{W}_2^N(m_2^t) \in \mathbb{C}^{L_2^+ \times N}$.

In block t , knowing the past bin index ℓ^{t-1} , node 1 transmits

$$\mathbf{X}_1^N = \mathbf{\Lambda}_a \mathbf{U}^N(\ell^{t-1}) + \mathbf{\Lambda}_b \tilde{\mathbf{V}}^N(m_{10}^t) + \mathbf{\Lambda}_c \mathbf{W}_1^N(m_{11}^t). \quad (39)$$

In block t , after recovering $\hat{\ell}^{t-1}$ from the previous block $t-1$, node 2 transmits

$$\mathbf{X}_2^N = \mathbf{\Lambda}_d \mathbf{U}^N(\hat{\ell}^{t-1}) + \mathbf{\Lambda}_e \mathbf{W}_2^N(m_2^t). \quad (40)$$

The decoding is similar to the proof of Proposition 1. ■

We now evaluate the converse of Theorem 2 for the vector Gaussian channel. First, two useful lemmas are stated below.

Lemma 1 (Lemma 3.1 in [22]): For two arbitrary complex random vectors $\mathbf{a}, \mathbf{b} \in \mathbb{C}^m$, it holds true that

$$\mathbf{K}_{11} - \mathbf{K}_{12} \mathbf{K}_{22}^{-1} \mathbf{K}_{12}^H \preceq \mathbf{K}_{11}, \quad (41)$$

where $\mathbf{K}_{ij} = \mathbb{E}(\mathbf{a}_i \mathbf{a}_j^H)$.

Lemma 2 (Lemma 3.2 in [22]): For two arbitrary random vectors $\mathbf{a}, \mathbf{b} \in \mathbb{C}^m$, it holds true that

$$\mathbb{E}(\mathbf{a} \mathbf{b}^H + \mathbf{b} \mathbf{a}^H) \preceq \mathbb{E} \left(\frac{1}{\tau} \mathbf{a} \mathbf{b}^H + \tau \mathbf{b} \mathbf{a}^H \right) \quad (42)$$

given any $\tau > 0$.

With the aid of the above two lemmas, we can derive a closed-form outer bound from the full mutual information converse (9), as stated in the following proposition.

Proposition 6: For the vector Gaussian channel, any achievable rate pair (R_1, R_2) must satisfy

$$R_1 \leq \log \left| \mathbf{I} + \frac{P_1}{\sigma^2} \mathbf{G}_{21} \mathbf{G}_{21}^H \right|, \quad (43a)$$

$$R_2 \leq \log \left| \mathbf{I} + \frac{P_2}{\sigma^2} \mathbf{G}_{32} \mathbf{G}_{32}^H \right|, \quad (43b)$$

$$\begin{aligned} R_1 + R_2 &\leq \log \left| \mathbf{I} + \mathbf{G}_{21} \left(\frac{\sigma^2}{P_1} \mathbf{I} + \mathbf{G}_{31}^H \mathbf{G}_{31} \right)^{-1} \mathbf{G}_{21}^H \right| + \\ &\quad \log \left| \mathbf{I} + \frac{2}{\sigma^2} (P_1 \mathbf{G}_{31} \mathbf{G}_{31}^H + P_2 \mathbf{G}_{32} \mathbf{G}_{32}^H) \right|. \end{aligned} \quad (43c)$$

Proof: Starting from (15a), we have

$$\begin{aligned} R_1 &\leq I(\mathbf{X}_1; \mathbf{Y}_2 | \mathbf{X}_2) \\ &= h(\mathbf{Y}_2 | \mathbf{X}_2) - h(\mathbf{Z}_2) \\ &\leq \log \left| \frac{1}{\sigma^2} \text{Var}(\mathbf{Y}_2 | \mathbf{X}_2) \right|. \end{aligned} \quad (44)$$

We further show that

$$\begin{aligned} \text{Var}(\mathbf{Y}_2 | \mathbf{X}_2) &\preceq \mathbb{E}(\mathbf{Y}_2 \mathbf{Y}_2^H) - \mathbb{E}(\mathbf{Y}_2 \mathbf{X}_2^H) \mathbb{E}^{-1}(\mathbf{X}_2 \mathbf{X}_2^H) \mathbb{E}(\mathbf{X}_2 \mathbf{Y}_2^H) \\ &= \sigma^2 \mathbf{I} + \mathbb{E}(\mathbf{G}_{21} \mathbf{X}_1 \mathbf{X}_1^H \mathbf{G}_{21}^H) \\ &\quad - \mathbb{E}(\mathbf{G}_{21} \mathbf{X}_1 \mathbf{X}_2^H) \mathbb{E}^{-1}(\mathbf{X}_2 \mathbf{X}_2^H) \mathbb{E}(\mathbf{X}_2 \mathbf{X}_2^H \mathbf{G}_{21}^H) \\ &\stackrel{(a)}{\preceq} \sigma^2 \mathbf{I} + \mathbb{E}(\mathbf{G}_{21} \mathbf{X}_1 \mathbf{X}_1^H \mathbf{G}_{21}^H) \\ &\stackrel{(b)}{\preceq} \sigma^2 \mathbf{I} + P_1 \mathbf{G}_{21} \mathbf{G}_{21}^H, \end{aligned} \quad (45)$$

where (a) follows by Lemma 1 and (b) follows by Hadamard's inequality. Incorporating (45) into (44) gives (43a). The upper bound (43b) on R_2 can be obtained similarly.

Regarding $R_1 + R_2$, we show that

$$\begin{aligned}
R_1 + R_2 &\leq I(\mathbf{X}_1; \mathbf{Y}_2, \mathbf{Y}_3 | \mathbf{X}_2) + I(\mathbf{X}_2; \mathbf{Y}_3) \\
&\leq \log \left| \frac{1}{\sigma^2} \text{Var}(\mathbf{Y}_3) \right| + \log \left| \frac{1}{\sigma^2} \text{Var}(\mathbf{Y}_2 | \mathbf{X}_2, \mathbf{Y}_3) \right| \\
&\stackrel{(c)}{\leq} \log \left| \mathbf{I} + \frac{2}{\sigma^2} (P_1 \mathbf{G}_{31} \mathbf{G}_{31}^H + P_2 \mathbf{G}_{32} \mathbf{G}_{32}^H) \right| \\
&\quad + \log \left| \frac{1}{\sigma^2} \text{Var}(\mathbf{Y}_2 | \mathbf{X}_2, \mathbf{Y}_3) \right|, \tag{46}
\end{aligned}$$

where (c) follows by Lemma 2 with $\tau = 1$. Letting $\mathbf{K}_{1|2} = \text{Var}(\mathbf{X}_1 | \mathbf{X}_2)$, we further show that

$$\begin{aligned}
&\text{Var}(\mathbf{Y}_2 | \mathbf{X}_2, \mathbf{Y}_3) \\
&= \text{Var}(\mathbf{Z}_2) + \text{Var}(\mathbf{G}_{21} \mathbf{X}_1 | \mathbf{X}_2, \mathbf{Y}_3) \\
&\preceq \sigma^2 \mathbf{I} + \mathbf{G}_{21} \mathbf{K}_{1|2} \mathbf{G}_{21}^H \\
&\quad - \mathbf{G}_{21} \mathbf{K}_{1|2} \mathbf{G}_{31}^H (\sigma^2 \mathbf{I} + \mathbf{G}_{31} \mathbf{K}_{1|2} \mathbf{G}_{31}^H)^{-1} \mathbf{G}_{31} \mathbf{K}_{1|2} \mathbf{G}_{21}^H \\
&\stackrel{(d)}{=} \sigma^2 \mathbf{I} + \mathbf{G}_{21} \left(\mathbf{K}_{1|2}^{-1} + \frac{1}{\sigma^2} \mathbf{G}_{31}^H \mathbf{G}_{31} \right)^{-1} \mathbf{G}_{21}^H \\
&\preceq \sigma^2 \mathbf{I} + \mathbf{G}_{21} \left(\frac{1}{P_1} \mathbf{I} + \frac{1}{\sigma^2} \mathbf{G}_{31}^H \mathbf{G}_{31} \right)^{-1} \mathbf{G}_{21}^H, \tag{47}
\end{aligned}$$

where (d) is due to the Woodbury matrix identity. Combining (46) and (47) yields (43c). ■

Based on the above pair of inner and outer bounds, we can determine an approximate capacity region of the FD cellular network with multiple antennas at each node.

Theorem 4: For the vector Gaussian channel, the achievable region of (R_1, R_2) as in Proposition 5 is within a constant gap δ bits/s/Hz to the capacity region, where

$$\delta = \max \left\{ \min\{L_1^+, L_2^-\}, \min\{L_2^+, L_3^-\}, \frac{1}{2} \min\{L_1^+, L_3^-\} \right\}. \tag{48}$$

Proof: We set $\mathbf{\Lambda}_a = \mathbf{\Lambda}_d = \mathbf{0}$, $\mathbf{\Lambda}_c = (\frac{\sigma^2}{P_1} \mathbf{I} + \mathbf{G}_{31}^H \mathbf{G}_{31})^{-\frac{1}{2}}$, $\mathbf{\Lambda}_b = (P_1 \mathbf{I} - \mathbf{\Sigma}_c)^{\frac{1}{2}}$, and $\mathbf{\Lambda}_e = \sqrt{P_2} \mathbf{I}$ in (37). The above constant gap can be obtained by comparing (37) and (43) under this setting. ■

IV. CAPACITY LIMITS OF FD CELLULAR NETWORK WITH D2D

We now include a direct D2D transmission of m_3 from the uplink user (node 1) to the downlink user (node 3). As before, we begin with the discrete memoryless model, then specialize the results to the scalar Gaussian model and the vector Gaussian model. The main contribution of this section is the capacity region of the scalar Gaussian channel to within a constant gap.

A. Achievability for Discrete Memoryless Channel with D2D

We use the existing works [9], [10] on the relay broadcast channel as a starting point. The works [9], [10] propose to modify the classic Marton's coding [7] for the broadcast channel to the case where one receiver further helps the other receiver via a relay link. The channel model considered in this paper is a further generalization in which the extra side message m_2 is carried in this relay link. The coding strategy proposed below incorporates m_2 in the Marton's coding.

The coding strategy of [9], [10] splits each message (i.e., m_1 and m_3) into the private and common parts which are dealt with differently. The common part is decoded by both node 2 and node 3; node 2 further acts as a relay to assist node 3 in decoding the common message. In contrast, the private parts are decoded only by the intended node through the broadcast channel without using node 2 as relay, so the Marton's coding can be applied. This paper makes two modifications to this strategy in order to enable an extra transmission of m_2 . First, we let X_2 be encoded based on both m_1 and m_2 . Second, we let node 3 decode the original common and private message jointly with the new message m_2 . The resulting achievable rate region is stated below.

Theorem 5: For the discrete memoryless channel with D2D, a rate triple (R_1, R_2, R_3) is achievable if it is in the convex hull of

$$R_1 \leq \pi_3, \tag{49a}$$

$$R_2 \leq \min\{\pi_5, \pi_2 + \pi_6 - \pi_1\}, \tag{49b}$$

$$R_1 + R_3 \leq \pi_3 + \pi_4 - \pi_1, \tag{49c}$$

$$R_2 + R_3 \leq \pi_7, \tag{49d}$$

$$R_1 + R_2 + R_3 \leq \min\{\pi_2 + \pi_7 - \pi_1, \pi_3 + \pi_6 - \pi_1\}, \tag{49e}$$

for some $p(u)p(v, w_1, w_3, x_1 | u)p(x_2 | u)$ under the constraint that $\pi_1 \leq \pi_2 + \pi_4$, where

$$\pi_1 = I(W_1; W_3 | U, V), \tag{50a}$$

$$\pi_2 = I(W_1; Y_2 | U, V, X_2), \tag{50b}$$

$$\pi_3 = I(V, W_1; Y_2 | U, X_2), \tag{50c}$$

$$\pi_4 = I(W_3; Y_3 | U, V, X_2), \tag{50d}$$

$$\pi_5 = I(X_2; Y_3 | U, V, W_3), \tag{50e}$$

$$\pi_6 = I(W_3, X_2; Y_3 | U, V), \tag{50f}$$

$$\pi_7 = I(U, V, W_3, X_2; Y_3). \tag{50g}$$

Proof: Split m_i into the common-private message pair $(m_{i0}, m_{ii}) \in [1 : 2^{nR_{i0}}] \times [1 : 2^{nR_{ii}}]$ for $i \in \{1, 3\}$. Introduce a total of T blocks for block-Markov coding. For each block $t \in [1 : T]$, in an i.i.d. manner according to their respective distributions, generate a common codebook

- Relay codebook $\mathbf{u}^N(m_{10}^{t-1}, m_{30}^{t-1})$;
- Common codebook $\mathbf{v}^N(m_{10}^t, m_{30}^t | m_{10}^{t-1}, m_{30}^{t-1})$;
- Separate binning codebooks $\mathbf{w}_1^N(\ell_{11})$ and $\mathbf{w}_3^N(\ell_{33})$;
- Joint binning codebook $\mathbf{x}_1^N(\ell_{11}^t, \ell_{33}^t | m_{10}^{t-1}, m_{30}^{t-1})$;
- Downlink codebook $\mathbf{x}_2^N(m_{20}^t | m_{10}^{t-1}, m_{30}^{t-1})$,

where the codebook pair $(\mathbf{w}_1^N(\ell_{11}), \mathbf{w}_3^N(\ell_{33}))$ is for $(\ell_{11}, \ell_{33}) \in [1 : 2^{NR'_{11}}] \times [1 : 2^{NR'_{11}}]$, with $R'_{ii} \geq R_{ii}$, $i \in \{1, 3\}$, and with each ℓ_{ii} uniformly mapped to the bin of m_{ii} , i.e., $m_{ii} = \mathcal{B}_i(\ell_{ii})$.

In block t , node 1 finds a pair of $(\ell_{11}^t, \ell_{33}^t)$ such that $m_{1i}^t = \mathcal{B}_i(\ell_{1i}^t)$ for $i \in \{1, 3\}$ and that $(\mathbf{w}_1^N(\ell_{11}^t), \mathbf{w}_3^N(\ell_{33}^t))$ is *strongly typical*, then transmits $\mathbf{x}_1^N(\ell_{11}^t, \ell_{33}^t | m_{10}^{t-1}, m_{30}^{t-1})$. This encoding is guaranteed to be successful provided that

$$R'_{11} + R'_{33} - R_{11} - R_{33} \geq I(W_1; W_3 | U, V). \tag{51}$$

In block t , after obtaining $(\hat{m}_{10}^{t-1}, \hat{m}_{30}^{t-1})$ from the previous block $t - 1$, node 2 transmits $\mathbf{x}_2^N(m_{20}^t | \hat{m}_{10}^{t-1}, \hat{m}_{30}^{t-1})$, and

TABLE III
PROPOSED CODING SCHEME FOR THE D2D CASE WITH D2D RATE SPLITTING.

t	1	2	\dots	$T-1$	T
X_1	$\mathbf{x}_1^N(m_1^1, m_{30}^1, m_{33}^1 1, 1)$	$\mathbf{x}_1^N(m_1^2, m_{30}^2, m_{33}^2 m_1^1, m_{30}^1)$	\rightarrow	$\mathbf{x}_1^N(m_1^{T-1}, m_{30}^{T-1}, m_{33}^{T-1} m_1^{T-2}, m_{30}^{T-2})$	$\mathbf{x}_1^N(1, 1, 1 m_1^{T-1}, m_{30}^{T-1})$
Y_2	$(\hat{m}_1^1, \hat{m}_{30}^1, \hat{m}_{33}^1)$	$(\hat{m}_1^2, \hat{m}_{30}^2, \hat{m}_{33}^2)$	\rightarrow	$(\hat{m}_1^{T-1}, \hat{m}_{30}^{T-1}, \hat{m}_{33}^{T-1})$	\emptyset
X_2	$\mathbf{x}_2^N(m_2^1 1, 1)$	$\mathbf{x}_2^N(m_2^2 \hat{m}_1^1, \hat{m}_{30}^1)$	\rightarrow	$\mathbf{x}_2^N(m_2^{T-1} \hat{m}_1^{T-2}, \hat{m}_{30}^{T-2})$	$\mathbf{x}_2^N(m_2^T \hat{m}_1^{T-1}, \hat{m}_{30}^{T-1})$
Y_3	$(1, \hat{m}_2^1, 1, \hat{m}_{33}^1)$	$(\hat{m}_1^1, \hat{m}_2^2, \hat{m}_{30}^2, \hat{m}_{33}^2)$	\leftarrow	$(\hat{m}_1^{T-2}, \hat{m}_2^{T-1}, \hat{m}_{30}^{T-2}, \hat{m}_{33}^{T-1})$	$(\hat{m}_1^{T-1}, \hat{m}_2^T, \hat{m}_{30}^{T-1}, 1)$

TABLE IV
PROPOSED CODING SCHEME FOR THE D2D CASE WITH UPLINK RATE SPLITTING.

t	1	2	\dots	$T-1$	T
X_1	$\mathbf{x}_1^N(m_{10}^1, m_{11}^1, m_3^1 1, 1)$	$\mathbf{x}_1^N(m_{10}^2, m_{11}^2, m_3^2 m_{10}^1, m_{11}^1)$	\rightarrow	$\mathbf{x}_1^N(m_{10}^{T-1}, m_{11}^{T-1}, m_3^{T-1} m_{10}^{T-2}, m_{11}^{T-2})$	$\mathbf{x}_1^N(1, 1, 1 m_{10}^{T-1}, m_{11}^{T-1})$
Y_2	$(\hat{m}_{10}^1, \hat{m}_{11}^1, \hat{m}_3^1)$	$(\hat{m}_{10}^2, \hat{m}_{11}^2, \hat{m}_3^2)$	\rightarrow	$(\hat{m}_{10}^{T-1}, \hat{m}_{11}^{T-1}, \hat{m}_3^{T-1})$	\emptyset
X_2	$\mathbf{x}_2^N(m_2^1 1, 1)$	$\mathbf{x}_2^N(m_2^2 \hat{m}_{10}^1, \hat{m}_{11}^1)$	\rightarrow	$\mathbf{x}_2^N(m_2^{T-1} \hat{m}_{10}^{T-2}, \hat{m}_{11}^{T-2})$	$\mathbf{x}_2^N(m_2^T \hat{m}_{10}^{T-1}, \hat{m}_{11}^{T-1})$
Y_3	$(1, \hat{m}_2^1, 1)$	$(\hat{m}_{10}^1, \hat{m}_2^2, \hat{m}_3^2)$	\leftarrow	$(\hat{m}_{10}^{T-2}, \hat{m}_2^{T-1}, \hat{m}_3^{T-2})$	$(\hat{m}_{10}^{T-1}, \hat{m}_2^T, \hat{m}_3^{T-1})$

recovers $(\hat{m}_{10}^t, \hat{m}_{30}^t)$ jointly from the received signal \mathbf{y}_2^N ; this decoding is successful if

$$R'_{11} \leq I(W_1; Y_2 | U, V, X_2), \quad (52)$$

$$R_{10} + R_{30} + R'_{11} \leq I(V, W_1; Y_2 | U, X_2). \quad (53)$$

Node 3 decodes the blocks in a backward direction (unlike the sliding window decoding scheme of [10]), i.e., block $t-1$ prior to block t . In block t , after obtaining $(\hat{m}_{10}^t, \hat{m}_{30}^t)$ from the previous block $t+1$, node 1 recovers $(\hat{m}_{10}^t, \hat{m}_{30}^t, \hat{m}_{33}^t, \hat{m}_2^t)$ jointly; the following conditions guarantee a successful decoding:

$$R'_{33} \leq I(W_3; Y_3 | U, V, X_2), \quad (54)$$

$$R_2 \leq I(X_2; Y_3 | U, V, W_3), \quad (55)$$

$$R'_{33} + R_2 \leq I(W_3, X_2; Y_3 | U, V), \quad (56)$$

$$R_{10} + R_{30} + R'_{33} + R_2 \leq I(U, V, W_3, X_2; Y_3). \quad (57)$$

Combining (51)–(57) with $R_{11} \leq R'_{11}$, $R_{33} \leq R'_{33}$, $R_1 = R_{10} + R_{11}$, $R_3 = R_{30} + R_{33}$, and a nonnegative constraint on all the rate variables, and letting $T \rightarrow \infty$, we establish the proposed inner bound, including the constraint $\pi_1 \leq \pi_2 + \pi_4$, via the Fourier-Motzkin elimination. ■

Remark 6: Theorem 5 encompasses the following existing achievability results. It reduces to the inner bound of [9], [10] for the relay broadcast channel when $U = X_2$, and reduces to a decode-and-forward inner bound (9) of [4] for the same channel when $W_1 = W_3 = \emptyset$. Furthermore, it reduces to the inner bound of Theorem 1 for the no D2D case when $W_3 = \emptyset$.

Remark 7: The present paper and [9], [10] both incorporate the decode-and-forward relaying into the achievability, but in different ways. This work uses the backward coding scheme while [9], [10] use the sliding window coding scheme.

In Theorem 5, the term π_1 is due to Marton's coding [7], reflecting the extent to which the encodings of the private messages m_{11} and m_{33} are coordinated through broadcasting. The following proposition further shows that the constraint $\pi_1 \leq \pi_2 + \pi_4$ must be satisfied automatically if

$p(u)p(v, w_1, w_3, x_1 | u)p(x_2 | u)$ is optimally chosen for maximizing the rate region (49).

Proposition 7: The achievable rate region of Theorem 5 remains the same if the constraint $\pi_1 \leq \pi_2 + \pi_4$ is removed.

Proof: Let \mathcal{A}_1 be the achievable rate region of Theorem 5, and let \mathcal{A}_2 be the version without the constraint $\pi_1 \leq \pi_2 + \pi_4$. Clearly, $\mathcal{A}_1 \subseteq \mathcal{A}_2$, so it suffices to prove $\mathcal{A}_2 \subseteq \mathcal{A}_1$. Consider some $p(u)p(v, w_1, w_3, x_1 | u)p(x_2 | u)$ such that $\pi_1 > \pi_2 + \pi_4$. Under this probability mass function, it can be shown that $\mathcal{A}_2 \subseteq \mathcal{A}'_2$ where \mathcal{A}'_2 is

$$R_2 \leq \min\{\pi_5, I(X_2; Y_3 | U, V)\}, \quad (58a)$$

$$R_1 + R_3 \leq I(V; Y_2 | U, X_2), \quad (58b)$$

$$R_1 + R_2 + R_3 \leq I(U, V, X_2; Y_3). \quad (58c)$$

In the meanwhile, \mathcal{A}'_2 can be attained by setting $W_1 = \emptyset$ in Theorem 5. Thus, $\mathcal{A}_2 \subseteq \mathcal{A}_1$. ■

The inner bound of Theorem 5 involves rate splitting for both m_1 and m_3 . The following two corollaries present the special cases in which only one of (m_1, m_3) has rate splitting and Marton's coding is replaced with the superposition coding. It turns out that using one of the two special cases according to the channel condition can already achieve the capacity to within a constant gap for the Gaussian FD cellular network with D2D.

Corollary 1 (D2D Rate Splitting): For the discrete memoryless channel with D2D, the rate triple (R_1, R_2, R_3) is achievable if it is in the convex hull of

$$R_1 \leq I(V; Y_2 | U, X_2), \quad (59a)$$

$$R_2 \leq I(X_2; Y_3 | U, X_1), \quad (59b)$$

$$R_1 + R_3 \leq I(V; Y_2 | U, X_2) + I(X_1; Y_3 | U, V, X_2), \quad (59c)$$

$$R_1 + R_2 + R_3 \leq I(V; Y_2 | U, X_2) + I(X_1, X_2; Y_3 | U, V), \quad (59d)$$

$$R_1 + R_2 + R_3 \leq I(X_1, X_2; Y_3), \quad (59e)$$

$$R_1 \leq \min \left\{ C \left(\frac{(1-\rho^2)|g_{21}|^2 P_1}{\sigma^2 + \alpha(1-\rho^2)|g_{21}|^2 P_1} \right), C \left(\frac{\beta(1-\rho^2)|g_{21}|^2 P_1}{\sigma^2} \right) \right\}, \quad (62a)$$

$$R_2 \leq C \left(\frac{(1-\rho^2)|g_{32}|^2 P_2}{\sigma^2} \right), \quad (62b)$$

$$R_3 \leq \min \left\{ C \left(\frac{\alpha(1-\rho^2)(|g_{21}|^2 + |g_{31}|^2) P_1}{\sigma^2} \right), C \left(\frac{(1-\rho^2)(|g_{21}|^2 + |g_{31}|^2) P_1}{\sigma^2 + \beta(1-\rho^2)(|g_{21}|^2 + |g_{31}|^2) P_1} \right) \right\}, \quad (62c)$$

$$R_1 + R_3 \leq C \left(\frac{(1-\rho^2)(|g_{21}|^2 + |g_{31}|^2) P_1}{\sigma^2} \right), \quad (62d)$$

$$R_2 + R_3 \leq C \left(\frac{|g_{31}|^2 P_1 + |g_{32}|^2 P_2 + J\rho}{\sigma^2} \right), \quad (62e)$$

$$R_1 + R_2 + R_3 \leq C \left(\frac{|g_{31}|^2 P_1 + |g_{32}|^2 P_2 + J\rho}{\sigma^2} \right) + C \left(\frac{(1-\rho^2)g_{21}^2 P_1}{\sigma^2 + (1-\rho^2)g_{31}^2 P_1} \right). \quad (62f)$$

for some pmf $p(u)p(v, x_1|u)p(x_2|u)$.

Proof: This inner bound is obtained by setting $W_1 = \emptyset$ and $W_3 = X_1$ in (49). The corresponding encoding and decoding procedure is illustrated in Tabel III. ■

Corollary 2 (Uplink Rate Splitting): For the discrete memoryless channel with D2D, a rate triple (R_1, R_2, R_3) is achievable if it is contained in the convex hull of

$$R_2 \leq I(X_2; Y_3|U, V), \quad (60a)$$

$$R_1 + R_3 \leq I(X_1; Y_2|U, X_2), \quad (60b)$$

$$R_2 + R_3 \leq I(U, V, X_2; Y_3), \quad (60c)$$

$$R_1 + R_2 + R_3 \leq I(X_1; Y_2|U, V, X_2) + I(U, V, X_2; Y_3), \quad (60d)$$

for some pmf $p(u)p(v, x_1|u)p(x_2|u)$.

Proof: This inner bound is obtained by setting $W_3 = \emptyset$ and $W_1 = X_1$ in (49). The corresponding encoding and decoding procedure is illustrated in Tabel IV. ■

B. Converse for Discrete Memoryless Channel with D2D

The existing works [9], [10] on the relay broadcast channel use auxiliary “genie” variables to improve the cut-set bound. Similarly, with the aid of genie, [8] enhances the cut-set bound for the case with relay-to-destination side message. As compared to [8], we provide two improvements. First, we further tighten the genie-aided bound by using more suitable auxiliary variables. Second, we propose a new upper bound on $R_1 + R_2 + R_3$ that improves the cut-set bound. Our converse is specified in the following.

Theorem 6: For the discrete memoryless channel with D2D, any achievable rate triple (R_1, R_2, R_3) must be in the convex hull of

$$R_1 \leq I(U; Y_2|X_2), \quad (61a)$$

$$R_1 \leq I(X_1; Y_2, Y_3|V, X_2), \quad (61b)$$

$$R_2 \leq I(X_2; Y_3|X_1), \quad (61c)$$

$$R_3 \leq I(X_1; Y_2, Y_3|U, X_2), \quad (61d)$$

$$R_3 \leq I(V; Y_2, Y_3|X_2), \quad (61e)$$

$$R_1 + R_3 \leq I(X_1; Y_2, Y_3|X_2), \quad (61f)$$

$$R_2 + R_3 \leq I(X_1, X_2; Y_3), \quad (61g)$$

$$R_1 + R_2 + R_3 \leq I(X_1; Y_2, Y_3|X_2) + I(X_2; Y_3), \quad (61h)$$

for some $p(u, v, x_1, x_2)$.

Proof: Observe that (61c), (61f) and (61g) are directly from the cut-set bound. The rest of the bound except (61h) is based on the auxiliary variables U and V . The existing work [8] assumes a genie that provides $U_n = (\mathbf{Y}_2^{n-1}, \mathbf{Y}_3^{n-1})$ and $V_n = M_3$ to node 1 and node 2. In contrast, by letting $U_n = (M_1, M_2, \mathbf{Y}_2^{n-1}, \mathbf{Y}_3^{n-1})$ and $V_n = (M_2, M_3, \mathbf{Y}_2^{n-1}, \mathbf{Y}_3^{n-1})$, we propose a different genie that provides U_n to node 1 and node 3, and provides V_n to node 1 and node 2. This new use of genie yields a tighter outer bound.

Regarding (61h), the main idea is the following. Considering node 2 and node 3 as two receivers, we follow Sato’s approach in [23] and assume that they could fully coordinate in their decoding with the aid of genie. Considering node 2 as the transmitter of m_2 , we introduce a genie that provides feedback \mathbf{Y}_3^{n-1} to it to improve encoding. The converse is then established by letting $N \rightarrow \infty$. The complete proof is shown in Appendix A. ■

Remark 8: As compared to the previous work, the converse in [8] is not computable, while the converse of Theorem 6 can be evaluated for the Gaussian case as shown in the next section. We remark that the sum-rate bound (61h) is new; it is crucial for proving the approximate capacity result for the Gaussian case as shown in the next section.

C. Scalar Gaussian Channel with D2D

The main goal of this section is to determine the capacity region of the scalar Gaussian case to within a constant gap. First, we specialize the converse of Theorem 6 to the Gaussian case. The following outer bound is an evaluation of (61). The evaluation relies on the entropy power inequality and is nontrivial. Its proof is provided in Appendix B.

Proposition 8: Any achievable rate triple (R_1, R_2, R_3) of the scalar Gaussian channel with D2D is in the convex hull of (62), which is displayed at the top of the page, for some parameters $0 \leq \alpha, \beta, \rho \leq 1$.

For achievability, instead of evaluating the full mutual information bounds of Theorem 5, we propose two simpler schemes, corresponding to rate splitting of either m_1 or m_3 , that turn out to be sufficient for proving the constant-gap result.

Proposition 9 (D2D Rate Splitting): A rate triple (R_1, R_2, R_3) of the scalar Gaussian channel with D2D is achievable if it is in the convex hull of

$$R_1 \leq C\left(\frac{b|g_{21}|^2 P_1}{\sigma^2 + c|g_{21}|^2 P_1}\right), \quad (63a)$$

$$R_2 \leq C(e|g_{32}|^2 P_2 / \sigma^2), \quad (63b)$$

$$R_1 + R_3 \leq C\left(\frac{b|g_{21}|^2 P_1}{\sigma^2 + c|g_{21}|^2 P_1}\right) + C\left(\frac{c|g_{31}|^2 P_1}{\sigma^2}\right), \quad (63c)$$

$$R_1 + R_2 + R_3 \leq C\left(\frac{b|g_{21}|^2 P_1}{\sigma^2 + c|g_{21}|^2 P_1}\right) + C\left(\frac{c|g_{31}|^2 P_1 + e|g_{32}|^2 P_2}{\sigma^2}\right), \quad (63d)$$

$$R_1 + R_2 + R_3 \leq C\left(\frac{|g_{31}|^2 P_1 + |g_{32}|^2 P_2 + J\sqrt{ad}}{\sigma^2}\right), \quad (63e)$$

for some $a, b, c, d, e \geq 0$ with $a + b + c = 1$ and $d + e = 1$.

Proof: Splitting only m_3 into (m_{30}, m_{33}) , we treat (m_1, m_{30}) as the common part to be decoded at both node 2 and node 3. The codebooks $\mathbf{w}_2^N(m_2)$, $\mathbf{w}_3^N(m_{33})$, $\check{\mathbf{v}}^N(m_1, m_{30})$, and $\mathbf{u}^N(m_1, m_{30})$ are generated randomly and independently according to $\mathcal{CN}(0, 1)$. In block $t \in [1 : T]$, node 1 transmits

$$\mathbf{x}_1^N(t) = \mathbf{v}^N(t) + \sqrt{cP_1}\mathbf{w}_3^N(m_{33}^t), \quad (64)$$

where

$$\mathbf{v}^N(t) = \sqrt{aP_1}\mathbf{u}^N(m_1^{t-1}, m_{30}^{t-1}) + \sqrt{bP_1}\check{\mathbf{v}}^N(m_1^t, m_{30}^t). \quad (65)$$

In block t , with $(\hat{m}_1^{t-1}, \hat{m}_{30}^{t-1})$ obtained from the previous block $t-1$, node 2 transmits

$$\mathbf{x}_2^N(t) = \sqrt{dP_2}\mathbf{u}^N(\hat{m}_1^{t-1}, \hat{m}_{30}^{t-1}) + \sqrt{eP_2}\mathbf{w}_2^N(m_2^t). \quad (66)$$

Using the decoding strategy of Theorem 5 establishes the proposed achievability result. ■

Alternatively, we can split m_1 to obtain the following inner bound. Full proof is omitted here.

Proposition 10 (Uplink Rate Splitting): A rate triple (R_1, R_2, R_3) of the scalar Gaussian channel with D2D is achievable if it is in the convex hull of

$$R_2 \leq C\left(\frac{e|g_{32}|^2 P_2}{\sigma^2 + c|g_{31}|^2 P_1}\right), \quad (67a)$$

$$R_1 + R_3 \leq C\left(\frac{(b+c)|g_{21}|^2 P_1}{\sigma^2}\right), \quad (67b)$$

$$R_2 + R_3 \leq C\left(\frac{(a+b)|g_{31}|^2 P_1 + |g_{32}|^2 P_2 + J\sqrt{ad}}{\sigma^2 + c|g_{31}|^2 P_1}\right), \quad (67c)$$

$$R_1 + R_2 + R_3 \leq C\left(\frac{c|g_{21}|^2 P_1}{\sigma^2}\right) + C\left(\frac{(a+b)|g_{31}|^2 P_1 + |g_{32}|^2 P_2 + J\sqrt{ad}}{\sigma^2 + c|g_{31}|^2 P_1}\right). \quad (67d)$$

for some $a, b, c, d, e \geq 0$ with $a + b + c = 1$ and $d + e = 1$.

We now have two achievable rate regions based on two different rate-splitting strategies. Suppose that the D2D channel

g_{31} is much stronger than the uplink channel g_{21} , we would let node 3 decode the entire m_1 for interference cancellation, so m_1 ought not to be split in this situation. Likewise, we would not split m_3 if g_{21} is much stronger. Hence, we propose to apply the D2D rate splitting strategy if $|g_{31}| \geq |g_{21}|$, and the uplink rate splitting strategy otherwise. This approach turns out to be approximately optimal.

Theorem 7: For the scalar Gaussian channel with D2D, the outer bound of Proposition 8 is at most 1 b/s/Hz from the inner bound of Proposition 9 if $|g_{31}| \geq |g_{21}|$, and at most 1 b/s/Hz from the inner bound of Proposition 10 if $|g_{31}| < |g_{21}|$. Thus, the achievability result of Theorem 5 and the converse result of Theorem 6 are within 1 b/s/Hz from each other for the scalar Gaussian case. This constant gap result carries over to the Gaussian relay broadcast channel of [9], [10].

Proof: We use the power splitting strategy of [21] to set $a = d = 0$, $b = 1 - c$, and $e = 1$, but to set c differently for the two strategies. We choose $c = \min\{1, |g_{21}|^2 P_1 / \sigma^2\}$ in Proposition 9, and choose $c = \min\{1, |g_{31}|^2 P_1 / \sigma^2\}$ in Proposition 10. The gap is established after some algebra. ■

Remark 9: To split rate differently depending on the channel condition is crucial in the above result; using either of the two strategies alone does give us a bounded gap.

D. Vector Gaussian Channel with D2D

This section examines the vector version of the Gaussian FD cellular network with D2D transmission. The superposition coding scheme that splits either m_1 or m_3 is no longer approximately optimal. We now consider splitting both of them. Our main results are three different achievable rate regions, all based on the dirty paper coding. First, the following lemma reviews the dirty paper coding.

Lemma 3 (Vector Writing on Dirty Paper): Consider a point-to-point vector Gaussian channel

$$\mathbf{Y} = \mathbf{G}\mathbf{X} + \mathbf{S} + \mathbf{Z} \quad (68)$$

with $\mathbf{Z} \sim \mathcal{CN}(\mathbf{0}, \sigma^2 \mathbf{I})$, the channel state variable $\mathbf{S} \sim \mathcal{CN}(\mathbf{0}, \tilde{\sigma}^2 \mathbf{I})$ noncausally available to the encoder of \mathbf{X} , and the power constraint P . Its capacity

$$C = \max_{\text{Tr}(\mathbf{K}_\mathbf{X}) \leq P} (I(\mathbf{W}; \mathbf{Y}) - I(\mathbf{W}; \mathbf{S})) \quad (69)$$

is attained by letting (i) $\mathbf{X} \perp \mathbf{S}$ and (ii) $\mathbf{W} = \mathbf{X} + \mathbf{Q}\mathbf{S}$ with

$$\mathbf{Q} = \mathbf{K}_\mathbf{X} \mathbf{G}^H (\sigma^2 \mathbf{I} + \mathbf{G} \mathbf{K}_\mathbf{X} \mathbf{G}^H)^{-1}, \quad (70)$$

where $\mathbf{K}_\mathbf{X} = \mathbf{X}\mathbf{X}^H$.

Since the two private messages m_{11} and m_{33} , which cause interference in the network, are both encoded at node 1, either of them can be used as a noncausal channel state information (i.e., the dirt) in the encoding of the other. Depending on what is treated as the dirt and what is treated as the background noise, there are three ways of performing dirty paper coding. First, we can treat m_{33} as the dirt in the encoding of m_{11} so that node 2 can decode m_{11} as if the interference from m_{33} does not exist. The uplink transmission has priority in this scheme. Second, we can treat m_{11} as the dirt in the encoding of m_{33} so that node 3 can decode m_{33} as if the interference

$$\Psi = (\mathbf{G}_{31}\mathbf{K}_d + \mathbf{G}_{31}\mathbf{K}_c\mathbf{G}_{31}^H\mathbf{Q}^H)(\mathbf{K}_d + \mathbf{Q}\mathbf{G}_{31}\mathbf{K}_c\mathbf{G}_{31}^H\mathbf{Q}^H)^{-1}(\mathbf{G}_{31}\mathbf{K}_d + \mathbf{G}_{31}\mathbf{K}_c\mathbf{G}_{31}^H\mathbf{Q}^H)^H. \quad (80)$$

from m_{11} does not exist; note here we assume that m_2 has been decoded and subtracted from \mathbf{Y}_3 . The D2D transmission has priority in this scheme. Third, we can still treat m_{11} as the dirt but treat m_2 as the noise in the encoding of m_{33} . This scheme aims to cancel the interference from (m_{11}, m_{33}) prior to the decoding of m_2 , so the downlink transmission has priority in this case. These three different ways of dirty paper coding are specified below.

Proposition 11 (Treating m_{33} as Dirt): For the vector Gaussian channel with D2D, a rate triple (R_1, R_2, R_3) is achievable if it is in the convex hull of (49) with

$$\pi_1 = \log \frac{|\mathbf{K}_c + \mathbf{Q}\mathbf{G}_{21}\mathbf{K}_d\mathbf{G}_{21}^H\mathbf{Q}^H|}{|\mathbf{K}_c|}, \quad (71a)$$

$$\pi_2 = \log |I + 1/\sigma^2 \cdot \mathbf{G}_{31}\mathbf{K}_c\mathbf{G}_{31}^H| + \pi_1, \quad (71b)$$

$$\pi_3 = \log \frac{|\sigma^2 I + \mathbf{G}_{21}(\mathbf{K}_b + \mathbf{K}_c + \mathbf{K}_d)\mathbf{G}_{21}^H|}{|\sigma^2 I + \mathbf{G}_{21}(\mathbf{K}_c + \mathbf{K}_d)\mathbf{G}_{21}^H|} + \pi_2, \quad (71c)$$

$$\pi_4 = \log \frac{|\sigma^2 I + \mathbf{G}_{31}(\mathbf{K}_c + \mathbf{K}_d)\mathbf{G}_{31}^H|}{|\sigma^2 I + \mathbf{G}_{31}\mathbf{K}_c\mathbf{G}_{31}^H|}, \quad (71d)$$

$$\pi_5 = \log \frac{|\sigma^2 I + \mathbf{G}_{31}\mathbf{K}_c\mathbf{G}_{31}^H + \mathbf{G}_{32}\mathbf{K}_f\mathbf{G}_{32}^H|}{|\sigma^2 I + \mathbf{G}_{31}\mathbf{K}_c\mathbf{G}_{31}^H|}, \quad (71e)$$

$$\pi_6 = \log \frac{|\sigma^2 I + \mathbf{G}_{31}(\mathbf{K}_c + \mathbf{K}_d)\mathbf{G}_{31}^H + \mathbf{G}_{32}\mathbf{K}_f\mathbf{G}_{32}^H|}{|\sigma^2 I + \mathbf{G}_{31}\mathbf{K}_c\mathbf{G}_{31}^H|}, \quad (71f)$$

$$\pi_7 = \log \frac{|\sigma^2 I + \Phi|}{|\sigma^2 I + \mathbf{G}_{31}\mathbf{K}_c\mathbf{G}_{31}^H|}, \quad (71g)$$

for some parameters $\Lambda_a \in \mathbb{C}^{L_1^+ \times \min\{L_1^+, L_2^+\}}$, $\Lambda_b \in \mathbb{C}^{L_1^+ \times L_1^+}$, $\Lambda_c \in \mathbb{C}^{L_1^+ \times L_1^+}$, $\Lambda_d \in \mathbb{C}^{L_1^+ \times L_1^+}$, $\Lambda_e \in \mathbb{C}^{L_2^+ \times \min\{L_1^+, L_2^+\}}$, $\Lambda_f \in \mathbb{C}^{L_2^+ \times L_2^+}$ with $\text{Tr}(\mathbf{K}_a + \mathbf{K}_b + \mathbf{K}_c + \mathbf{K}_d) \leq P_1$ and $\text{Tr}(\mathbf{K}_e + \mathbf{K}_f) \leq P_2$, where $\mathbf{K}_i = \Lambda_i \Lambda_i^H$, $\forall i \in \{a, b, c, d, e\}$,

$$\mathbf{Q} = \mathbf{K}_c\mathbf{G}_{21}^H(\sigma^2 I + \mathbf{G}_{21}\mathbf{K}_c\mathbf{G}_{21}^H)^{-1}, \quad (72)$$

and

$$\Phi = \mathbf{G}_{31}(\mathbf{K}_a + \mathbf{K}_b + \mathbf{K}_c + \mathbf{K}_d)\mathbf{G}_{31}^H + \mathbf{G}_{32}(\mathbf{K}_e + \mathbf{K}_f)\mathbf{G}_{32}^H + \mathbf{G}_{31}\Lambda_a\Lambda_e^H\mathbf{G}_{32}^H + \mathbf{G}_{32}\Lambda_e\Lambda_a^H\mathbf{G}_{31}^H. \quad (73)$$

Proof: Generate the following codebooks independently according to i.i.d. Gaussian distribution $\mathcal{CN}(0, I)$: Private codebook $\mathbf{D}_i(m_{ii}^t)$, $i \in \{1, 3\}$, common codebook $\tilde{\mathbf{V}}(m_{10}^t, m_{30}^t)$, relay codebook $\mathbf{U}(m_{10}^t, m_{30}^t)$, and downlink codebook $\mathbf{W}_2(m_2^t)$. Furthermore, treating $\Lambda_c\mathbf{D}_1$ as \mathbf{X} , $\mathbf{G}_{21}\Lambda_d\mathbf{D}_3$ as \mathbf{S} , and \mathbf{Z}_2 as \mathbf{Z} in Lemma 3, we set

$$\mathbf{W}_1(m_{11}^t, m_{33}^t) = \Lambda_c\mathbf{D}_1(m_{11}^t) + \mathbf{Q}\mathbf{G}_{21}\Lambda_d\mathbf{D}_3(m_{33}^t), \quad (74)$$

$$\mathbf{W}_3(m_{33}^t) = \Lambda_d\mathbf{D}_3(m_{33}^t). \quad (75)$$

In block t , node 1 transmits

$$\mathbf{X}_1 = \Lambda_a\mathbf{U}(m_{10}^{t-1}, m_{30}^{t-1}) + \Lambda_b\tilde{\mathbf{V}}(m_{10}^t, m_{30}^t) + \Lambda_c\mathbf{D}_1(m_{11}^t) + \Lambda_d\mathbf{D}_3(m_{33}^t), \quad (76)$$

and node 2 transmits

$$\mathbf{X}_2 = \Lambda_e\mathbf{U}(m_{10}^{t-1}, m_{30}^{t-1}) + \Lambda_f\mathbf{W}(m_2^t). \quad (77)$$

The primary idea to write m_{11} on the dirty paper of m_{33} , i.e.,

$$\mathbf{Y}_2 = \underbrace{\mathbf{G}_{21}(\Lambda_a\mathbf{U} + \Lambda_b\mathbf{V})}_{\text{Subtracted}} + \underbrace{\mathbf{G}_{21}\Lambda_c\mathbf{D}_1}_{\text{Signal}} + \underbrace{\mathbf{G}_{21}\Lambda_d\mathbf{D}_3}_{\text{Dirt}} + \mathbf{Z}_2, \quad (78)$$

where the first term can be directly subtracted from \mathbf{Y}_2 because node 2 already knows it when trying to decode m_{11}^t . The decoding part follows that as stated in the proof of Theorem 5. ■

Proposition 12 (Treating m_{11} as Dirt and Subtracting m_2 First): For the vector Gaussian channel with D2D, a rate triple (R_1, R_2, R_3) is achievable if it is in the convex hull of (49) with

$$\pi_1 = \log \frac{|\mathbf{K}_d + \mathbf{Q}\mathbf{G}_{31}\mathbf{K}_c\mathbf{G}_{31}^H\mathbf{Q}^H|}{|\mathbf{K}_d|}, \quad (79a)$$

$$\pi_2 = \log \frac{|\sigma^2 I + \mathbf{G}_{31}(\mathbf{K}_c + \mathbf{K}_d)\mathbf{G}_{31}^H|}{|\sigma^2 I + \mathbf{G}_{31}\mathbf{K}_d\mathbf{G}_{31}^H|}, \quad (79b)$$

$$\pi_3 = \log \frac{|\sigma^2 I + \mathbf{G}_{31}(\mathbf{K}_b + \mathbf{K}_c + \mathbf{K}_d)\mathbf{G}_{31}^H|}{|\sigma^2 I + \mathbf{G}_{31}\mathbf{K}_d\mathbf{G}_{31}^H|}, \quad (79c)$$

$$\pi_4 = \log |I + 1/\sigma^2 \cdot \mathbf{G}_{31}\mathbf{K}_d\mathbf{G}_{31}^H| + \pi_1, \quad (79d)$$

$$\pi_5 = \log \frac{|\sigma^2 I + \mathbf{G}_{31}(\mathbf{K}_c + \mathbf{K}_d)\mathbf{G}_{31}^H + \mathbf{G}_{32}\mathbf{K}_f\mathbf{G}_{32}^H|}{|\sigma^2 I + \mathbf{G}_{31}(\mathbf{K}_c + \mathbf{K}_d)\mathbf{G}_{31}^H|} + \pi_4$$

$$- \log \frac{|\sigma^2 I + \mathbf{G}_{31}(\mathbf{K}_c + \mathbf{K}_d)\mathbf{G}_{31}^H + \mathbf{G}_{32}\mathbf{K}_f\mathbf{G}_{32}^H|}{|\sigma^2 I + \mathbf{G}_{31}(\mathbf{K}_c + \mathbf{K}_d)\mathbf{G}_{31}^H + \mathbf{G}_{32}\mathbf{K}_f\mathbf{G}_{32}^H - \Psi|}, \quad (79e)$$

$$\pi_6 = \log \frac{|\sigma^2 I + \mathbf{G}_{31}(\mathbf{K}_c + \mathbf{K}_d)\mathbf{G}_{31}^H + \mathbf{G}_{32}\mathbf{K}_f\mathbf{G}_{32}^H|}{|\sigma^2 I + \mathbf{G}_{31}(\mathbf{K}_c + \mathbf{K}_d)\mathbf{G}_{31}^H|} + \pi_4,$$

$$\pi_7 = \log \frac{|\sigma^2 I + \Phi|}{|\sigma^2 I + \mathbf{G}_{31}(\mathbf{K}_c + \mathbf{K}_d)\mathbf{G}_{31}^H|} + \pi_4 - \pi_1, \quad (79f)$$

for some parameters $\Lambda_a \in \mathbb{C}^{L_1^+ \times \min\{L_1^+, L_2^+\}}$, $\Lambda_b \in \mathbb{C}^{L_1^+ \times L_1^+}$, $\Lambda_c \in \mathbb{C}^{L_1^+ \times L_1^+}$, $\Lambda_d \in \mathbb{C}^{L_1^+ \times L_1^+}$, $\Lambda_e \in \mathbb{C}^{L_2^+ \times \min\{L_1^+, L_2^+\}}$, $\Lambda_f \in \mathbb{C}^{L_2^+ \times L_2^+}$ with $\text{Tr}(\mathbf{K}_a + \mathbf{K}_b + \mathbf{K}_c + \mathbf{K}_d) \leq P_1$ and $\text{Tr}(\mathbf{K}_e + \mathbf{K}_f) \leq P_2$, where $\mathbf{K}_i = \Lambda_i \Lambda_i^H$, $\forall i \in \{a, b, c, d, e\}$, Φ is previously defined as in (73), Ψ is defined in (80) as displayed at the top of the page, and

$$\mathbf{Q} = \mathbf{K}_d\mathbf{G}_{31}^H(\sigma^2 I + \mathbf{G}_{31}\mathbf{K}_d\mathbf{G}_{31}^H)^{-1}. \quad (81)$$

Proof: All codebooks except \mathbf{W}_1 and \mathbf{W}_3 are the same as in the proof of Proposition 11. Assuming that the downlink signal has been subtracted from \mathbf{Y}_2 , we treat $\Lambda_d\mathbf{D}_3$ as \mathbf{X} , $\mathbf{G}_{31}\Lambda_c\mathbf{D}_1$ as \mathbf{S} , and \mathbf{Z}_3 as \mathbf{Z} in Lemma 3, thus setting

$$\mathbf{W}_1(m_{11}^t) = \Lambda_c\mathbf{D}_1(m_{11}^t), \quad (82)$$

$$\mathbf{W}_3(m_{11}^t, m_{33}^t) = \Lambda_d\mathbf{D}_3(m_{33}^t) + \mathbf{Q}\mathbf{G}_{31}\Lambda_c\mathbf{D}_1(m_{11}^t). \quad (83)$$

This dirty paper coding scheme can be illustrated as

$$\mathbf{Y}_3 = \underbrace{\mathbf{G}_{31}(\Lambda_a \mathbf{U} + \Lambda_b \mathbf{V})}_{\text{Subtracted}} + \underbrace{\mathbf{G}_{32} \mathbf{X}_2}_{\text{Dirt}} + \underbrace{\mathbf{G}_{31} \mathbf{D}_1}_{\text{Dirt}} + \underbrace{\mathbf{G}_{31} \mathbf{D}_3}_{\text{Signal}} + \mathbf{Z}_3. \quad (84)$$

As before, \mathbf{X}_1 is decided by (76) and \mathbf{X}_2 is decided by (77). The decoding procedure follows Theorem 5. ■

When m_{11} is treated as the dirt in the encoding of m_{33} , the other idea is to retain m_2 in the dirty paper coding. The resulting achievable rate region is stated below.

Proposition 13 (Treating m_{11} as Dirt and Treating m_2 as Noise): For the vector Gaussian channel with D2D, a rate triple (R_1, R_2, R_3) is achievable if it is in the convex hull of (49) with

$$\pi_1 = \log \frac{|\mathbf{K}_d + \mathbf{Q} \mathbf{G}_{31} \mathbf{K}_c \mathbf{G}_{31}^H \mathbf{Q}^H|}{|\mathbf{K}_d|}, \quad (85a)$$

$$\pi_2 = \log \frac{|\sigma^2 \mathbf{I} + \mathbf{G}_{31}(\mathbf{K}_c + \mathbf{K}_d) \mathbf{G}_{31}^H|}{|\sigma^2 \mathbf{I} + \mathbf{G}_{31} \mathbf{K}_d \mathbf{G}_{31}^H|}, \quad (85b)$$

$$\pi_3 = \log \frac{|\sigma^2 \mathbf{I} + \mathbf{G}_{31}(\mathbf{K}_b + \mathbf{K}_c + \mathbf{K}_d) \mathbf{G}_{31}^H|}{|\sigma^2 \mathbf{I} + \mathbf{G}_{31} \mathbf{K}_d \mathbf{G}_{31}^H|}, \quad (85c)$$

$$\pi_4 = \log \frac{|\sigma^2 \mathbf{I} + \mathbf{G}_{31}(\mathbf{K}_c + \mathbf{K}_d) \mathbf{G}_{31}^H|}{|\sigma^2 \mathbf{I} + \mathbf{G}_{31}(\mathbf{K}_c + \mathbf{K}_d) \mathbf{G}_{31}^H - \Psi|}, \quad (85d)$$

$$\pi_5 = \log \frac{|\sigma^2 \mathbf{I} + \mathbf{G}_{31}(\mathbf{K}_c + \mathbf{K}_d) \mathbf{G}_{31}^H + \mathbf{G}_{32} \mathbf{K}_f \mathbf{G}_{32}^H|}{|\sigma^2 \mathbf{I} + \mathbf{G}_{31}(\mathbf{K}_c + \mathbf{K}_d) \mathbf{G}_{31}^H|} + \pi_4 - \log \frac{|\sigma^2 \mathbf{I} + \mathbf{G}_{31} \mathbf{K}_d \mathbf{G}_{31}^H + \mathbf{G}_{32} \mathbf{K}_f \mathbf{G}_{32}^H|}{|\sigma^2 \mathbf{I} + \mathbf{G}_{32} \mathbf{K}_f \mathbf{G}_{32}^H|} - \pi_1, \quad (85e)$$

$$\pi_6 = \log \frac{|\sigma^2 \mathbf{I} + \mathbf{G}_{31}(\mathbf{K}_c + \mathbf{K}_d) \mathbf{G}_{31}^H + \mathbf{G}_{32} \mathbf{K}_f \mathbf{G}_{32}^H|}{|\sigma^2 \mathbf{I} + \mathbf{G}_{31}(\mathbf{K}_c + \mathbf{K}_d) \mathbf{G}_{31}^H|} + \pi_4, \quad (85f)$$

$$\pi_7 = \log \frac{|\sigma^2 \mathbf{I} + \Phi|}{|\sigma^2 \mathbf{I} + \mathbf{G}_{31}(\mathbf{K}_c + \mathbf{K}_d) \mathbf{G}_{31}^H|} + \pi_4 - \pi_1, \quad (85f)$$

for some parameters $\Lambda_a \in \mathbb{C}^{L_1^+ \times \min\{L_1^+, L_2^+\}}$, $\Lambda_b \in \mathbb{C}^{L_1^+ \times L_1^+}$, $\Lambda_c \in \mathbb{C}^{L_1^+ \times L_1^+}$, $\Lambda_d \in \mathbb{C}^{L_1^+ \times L_1^+}$, $\Lambda_e \in \mathbb{C}^{L_2^+ \times \min\{L_1^+, L_2^+\}}$, $\Lambda_f \in \mathbb{C}^{L_2^+ \times L_2^+}$ with $\text{Tr}(\mathbf{K}_a + \mathbf{K}_b + \mathbf{K}_c + \mathbf{K}_d) \leq P_1$ and $\text{Tr}(\mathbf{K}_e + \mathbf{K}_f) \leq P_2$, where $\mathbf{K}_i = \Lambda_i \Lambda_i^H$, $\forall i \in \{a, b, c, d, e\}$, Φ is previously defined as in (73), Ψ is previously defined in (80) as displayed at the top of the page, and

$$\mathbf{Q} = \mathbf{K}_d \mathbf{G}_{31}^H (\sigma^2 \mathbf{I} + \mathbf{G}_{32} \mathbf{K}_f \mathbf{G}_{32}^H + \mathbf{G}_{31} \mathbf{K}_d \mathbf{G}_{31}^H)^{-1}. \quad (86)$$

Proof: As compared to the coding scheme of the previous proposition, the only difference lies in the codebooks \mathbf{W}_1 and \mathbf{W}_2 which are now set as

$$\mathbf{W}_1(m_{11}^t) = \Lambda_c \mathbf{D}_1(m_{11}^t), \quad (87)$$

$$\mathbf{W}_3(m_{11}^t, m_{33}^t) = \Lambda_d \mathbf{D}_3(m_{33}^t) + \mathbf{Q} \mathbf{G}_{31} \Lambda_c \mathbf{D}_1(m_{11}^t). \quad (88)$$

We now treat $\Lambda_d \mathbf{D}_3$ as \mathbf{X} , $\mathbf{G}_{31} \Lambda_c \mathbf{D}_1$ as \mathbf{S} , and $\mathbf{Z}_3 +$

$\mathbf{G}_{32} \Lambda_f \mathbf{W}_2$ as \mathbf{Z} in Lemma 3, i.e.,

$$\mathbf{Y}_3 = \underbrace{\mathbf{G}_{31}(\Lambda_a \mathbf{U} + \Lambda_b \mathbf{V})}_{\text{Subtracted}} + \underbrace{\mathbf{G}_{32} \Lambda_e \mathbf{U}}_{\text{Dirt}} + \underbrace{\mathbf{G}_{31} \mathbf{D}_1}_{\text{Dirt}} + \underbrace{\mathbf{G}_{31} \mathbf{D}_3}_{\text{Signal}} + \mathbf{G}_{32} \Lambda_f \mathbf{W}_2 + \mathbf{Z}_3. \quad (89)$$

Again, \mathbf{X}_1 is decided by (76) and \mathbf{X}_2 is decided by (77). The decoding procedure is the same as for Theorem 5. ■

Remark 10: The use of Proposition 7 is critical in establishing and simplifying the above achievabilities.

Because of the difficulty in setting the auxiliary variables U and V of Theorem 6 for the vector Gaussian channel with D2D, we provide a converse based on the cut-set bound and the sum-rate bound (61h), as stated in the following proposition.

Proposition 14: For the vector Gaussian channel with D2D, any achievable rate triple (R_1, R_2, R_3) must be in the convex hull of

$$R_1 \leq \log \left| \mathbf{I} + \frac{P_1}{\sigma^2} \mathbf{G}_{21} \mathbf{G}_{21}^H \right| \quad (90a)$$

$$R_2 \leq \log \left| \mathbf{I} + \frac{P_1}{\sigma^2} \mathbf{G}_{32} \mathbf{G}_{32}^H \right|, \quad (90b)$$

$$R_3 \leq \log \left| \mathbf{I} + \frac{P_1}{\sigma^2} \mathbf{G}_{31} \mathbf{G}_{31}^H \right|, \quad (90c)$$

$$R_1 + R_3 \leq \log \left| \mathbf{I} + \frac{1}{\sigma^2} (\mathbf{G}_{31}^H \mathbf{K}_a \mathbf{G}_{31} + \mathbf{G}_{21}^H \mathbf{K}_b \mathbf{G}_{21}) \right|, \quad (90d)$$

$$R_2 + R_3 \leq \log \left| \mathbf{I} + \frac{2}{\sigma^2} (P_1 \mathbf{G}_{31} \mathbf{G}_{31}^H + P_2 \mathbf{G}_{32} \mathbf{G}_{32}^H) \right|, \quad (90e)$$

$$R_1 + R_2 + R_3 \leq \log \left| \mathbf{I} + \mathbf{G}_{21} \left(\frac{\sigma^2}{P_1} \mathbf{I} + \mathbf{G}_{31}^H \mathbf{G}_{31} \right)^{-1} \mathbf{G}_{21}^H \right| + \log \left| \mathbf{I} + \frac{2}{\sigma^2} (P_1 \mathbf{G}_{31} \mathbf{G}_{31}^H + P_2 \mathbf{G}_{32} \mathbf{G}_{32}^H) \right|, \quad (90f)$$

for some parameters $\mathbf{K}_a \in \mathbb{S}_+^{L_2^- \times L_2^-}$ and $\mathbf{K}_b \in \mathbb{S}_+^{L_3^- \times L_3^-}$ with $\text{Tr}(\mathbf{K}_a + \mathbf{K}_b) \leq P_1$.

Proof: First, (90a), (90b), (90c), and (90e) are directly from the cut-set bound. Furthermore, the maximum $R_1 + R_3$ equals to the maximum sum rate of a broadcast channel: $\mathbf{Y}_2 = \mathbf{G}_{21} \mathbf{X}_1 + \mathbf{Z}_2$ and $\mathbf{Y}_3 = \mathbf{G}_{31} \mathbf{X}_1 + \mathbf{Z}_3$, then can be evaluated by further applying a duality between the broadcast channel and the multiple access channel [24]; the bound (90d) is obtained thereafter. Finally, the bound (90f) on $R_1 + R_2 + R_3$ is an extension of the previous bound (62f). ■

We are unable to characterize the capacity region of the vector Gaussian case (R_1, R_2, R_3) to within a constant gap by using the above inner and outer bounds. Observe that the previous inner bounds (63) and (67) involve at most two logarithm terms in each inequality, whereas the inner bounds here involve more terms; this discrepancy makes it difficult to extend the constant-gap optimality of the scalar Gaussian channel to the vector Gaussian channel. In contrast, the no D2D case does not have this issue.

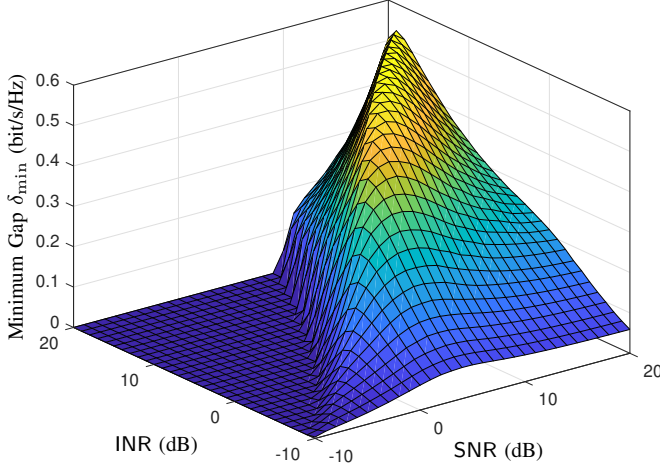


Fig. 3. Minimum gap δ_{\min} to the capacity region of (R_1, R_2) when $|g_{21}|^2 P_1 = |g_{32}|^2 P_2$.

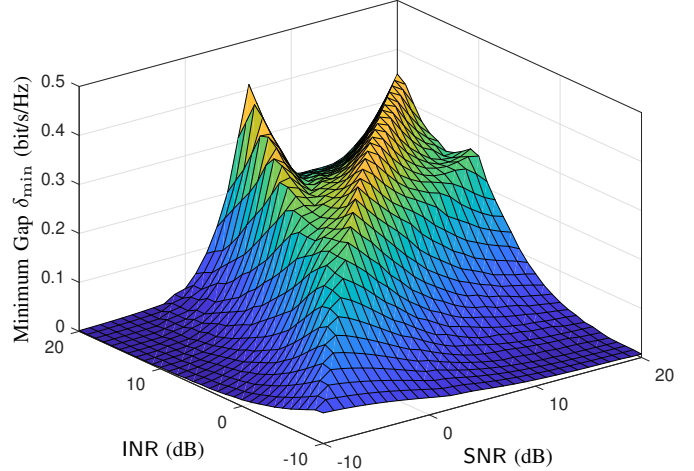


Fig. 5. Minimum gap δ_{\min} to the capacity region of (R_1, R_2, R_3) when $|g_{21}|^2 P_1 = |g_{32}|^2 P_2$.

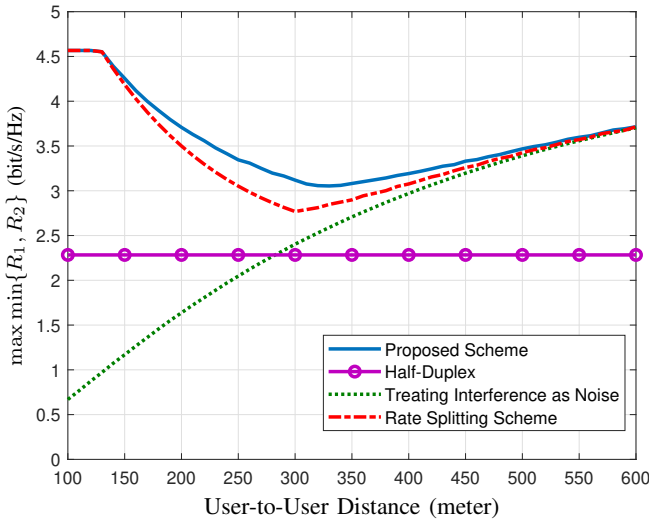


Fig. 4. Symmetric rate $\min\{R_1, R_2\}$ achieved by the different schemes when the user-to-BS distance is fixed at 300 meters.

V. NUMERICAL EXAMPLES

A. Without D2D Case

For the scalar Gaussian channel without D2D, Theorem 3 shows that the gap between our inner bound (17) and the capacity region is upper bounded by a constant $\delta = 1$ in general. This simulation aims to find the minimum possible gap δ_{\min} by optimizing the parameters (a, b, c, d, e) in (17) globally via exhaustive search. Assume that $|g_{21}|^2 P_1 = |g_{32}|^2 P_2$ and let $\text{SNR} = |g_{21}|^2 P_1 / \sigma^2$ and $\text{INR} = |g_{31}|^2 P_2 / \sigma^2$. Fig. 3 shows δ_{\min} with respect to the various (SNR, INR) pairs. According to the figure, our achievability yields a bigger gap to the capacity region when INR is close to SNR. Observe also that our inner bound and the capacity region coincide when INR is sufficiently higher than SNR; this observation agrees with Proposition 2.

We consider a FD cellular network in which the uplink/downlink user-to-BS distance is fixed at 300m, the user-to-user distance is set to different values. Let the maximum transmit power spectrum density (PSD) be -47 dBm/Hz for both uplink and downlink; we set the PSD of the background noise be -169 dBm/Hz. The channel magnitude is modeled as $-128.1 - 37.6 \log_{10}(\text{dist})$ in dB scale, where dist is the distance (in km). The following baselines are evaluated:

- Half-duplex with separate uplink and downlink;
- Treating interference as noise with FD uplink/downlink;
- Rate splitting scheme: The uplink message is split for interference cancellation, but without relaying by the BS.

Fig. 4 compares the symmetric uplink-downlink rate $\min\{R_1, R_2\}$ in the no D2D case. It shows that the proposed BS-aided scheme is more effective than simple interference cancellation, gaining up to about 0.5 bits/s/Hz. Observe that the proposed scheme shows the most benefit when the user-to-user distance is not too close or too far. Fig. 6 shows the trade-off between the D2D rate and the symmetric uplink-downlink rate when the two users are 300m apart. The proposed scheme achieves a larger rate region than the baseline schemes.

B. D2D Case

We now evaluate the minimum gap δ_{\min} for the D2D case of the scalar Gaussian channel. As before, assume $|g_{21}| = |g_{32}|$, and let $\text{SNR} = |g_{21}|^2 P_1 / \sigma^2$ and $\text{INR} = |g_{31}|^2 P_2 / \sigma^2$. Following Theorem 7, we choose the inner bound (63) if $\text{INR} \geq \text{SNR}$ and choose the inner bound (67) otherwise; parameters (a, b, c, d, e) are optimally determined by exhaustive search. Fig. 5 shows that the minimum gap between our achievability and the capacity is less than 0.5 bit/s/Hz, in contrast to the constant gap $\delta = 1$ given in Theorem 7. Fig. 5 shows two ridges which are due to the use of two different rate splitting schemes.

We further evaluate the data rates for a particular network setup as previously stated in the no D2D case. The three

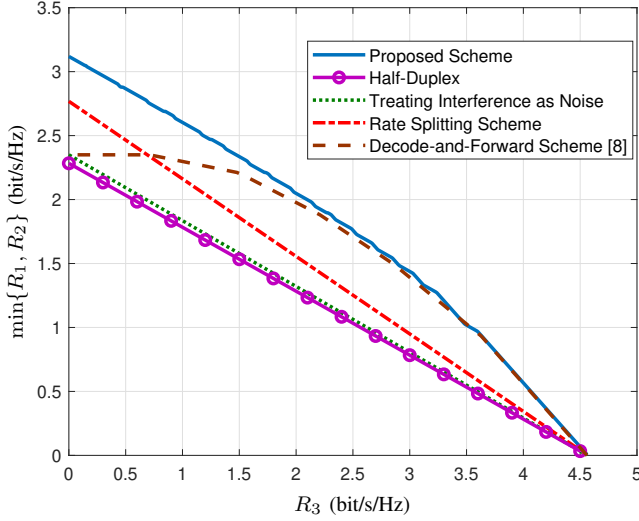


Fig. 6. R_3 vs. $\min\{R_1, R_2\}$ in the D2D case when users are 300m apart.

baselines are extended to the D2D case by time or frequency division multiplex of cellular and D2D traffic. In addition, we introduce a new benchmark called the decode-and-forward scheme—this corresponds to the scheme of [8]. Fig. 6 shows the trade-off between the D2D rate and the symmetric uplink-downlink rate when the two users are 300m apart. The proposed scheme achieves a larger rate region than the baseline schemes.

Finally, we compare the asymptotic behavior of the different schemes. We assume that $|g_{21}| = |g_{32}| = 1$ and $P_1 = P_2 = 1$; let $\text{SNR} = P_1/\sigma^2$ and $\text{INR} = |g_{31}|^2 P_2/\sigma^2$. Given a fixed ratio $\frac{\log \text{INR}}{\log \text{SNR}} = \kappa$, the symmetric general degree of freedom (GDoF) is defined as

$$d_{\text{sym}} \triangleq \lim_{\text{SNR} \rightarrow \infty} \frac{\min\{R_1, R_2, R_3\}}{\log \text{SNR}}. \quad (91)$$

Fig. 7 shows the symmetric GDoFs achieved by the different schemes. The GDoF of the proposed scheme equals to that of the capacity since the proposed scheme attains the capacity to within a constant gap. Observe that this optimal GDoF curve consists of four segments, i.e., $[0, 0.5)$, $[0.5, 1)$, $[1, 3)$, and $[3, \infty)$ with respect to κ . When $\kappa \in [0, 0.5)$, because the channel between node 1 and node 3 is so weak that it is useless in terms of GDoF, the optimal GDoF does not change with κ in this interval. When $\kappa \in [0.5, 1)$, the uplink rate splitting scheme of Proposition 10 attains the optimal GDoF. When $\kappa \in [1, 3)$, the D2D rate splitting scheme of Proposition 9 attains the optimal GDoF. Furthermore, when $\kappa \in [3, \infty)$, the channel between node 1 and node 3 is strong enough to let node 3 sequentially recover (m_1, m_2, m_3) by successive cancellation without relaying at the BS. In this situation, node 1 allocates power $P - P^{2-\kappa}$ to the transmission of m_1 and allocates power $P^{2-\kappa}$ to the transmission of m_3 , while node 2 transmits m_2 at the full power P . After subtracting the self-interference, node 2 removes m_3 and then decodes m_1 via the successive cancellation. Node 3 first decodes m_1 , then m_2 , and finally m_3 via the successive cancellation. As a result, each

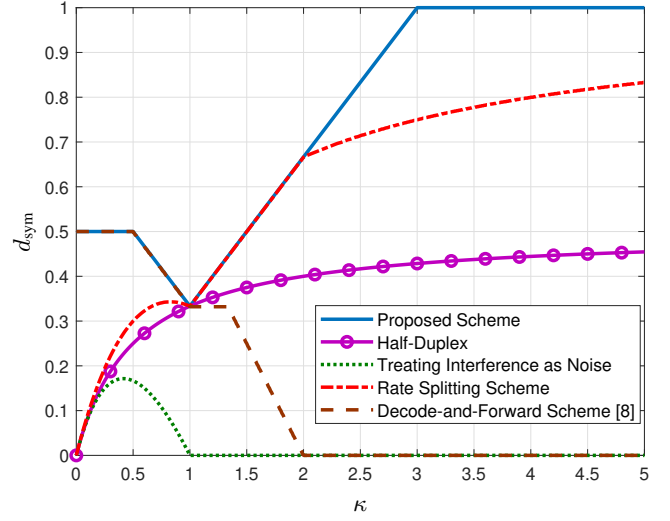


Fig. 7. Symmetric GDoF d_{sym} vs. parameter $\kappa = \frac{\log \text{INR}}{\log \text{SNR}}$ when $|g_{21}|^2 P_1 = |g_{32}|^2 P_2$.

transmission attains a GDoF of 1. Fig. 7 shows that all the other schemes are suboptimal in terms of GDoF.

VI. CONCLUSION

This paper aims to analyze the maximum possible transmission rates of the uplink message, the downlink message, and the D2D message in a wireless cellular network with the FD BS and two half-duplex user terminals. This FD cellular network can be modeled as a relay broadcast channel with side message. We propose new strategies to enlarge the existing achievable rate regions, a crucial component of which is to use the BS as a relay to facilitate cancelling interference. We further provide novel converse results that are strictly tighter than the cut-set bound and the state-of-the-art outer bound. Considering the uplink and downlink transmissions alone, we prove that our proposed schemes attain the capacity to within a constant gap for the Gaussian channel case, even when the BS and users are deployed with multiple antennas. Furthermore, if the D2D transmission is included, a constant-gap optimality is established for the scalar Gaussian channel case, which carries over to the relay broadcast channel. Three different ways of dirty paper coding are devised to deal with the vector Gaussian channel case.

APPENDIX A PROOF OF THEOREM 6

The set of inequalities (61c), (61f), and (61g) are the immediate results of the cut-set bound. The inequality of $R_1 + R_2 + R_3$ in (61h) is obtained by extending the sum-

rate outer bound of Theorem 2, as follows:

$$\begin{aligned}
& N(R_1 + R_2 + R_3 - \epsilon_N) \\
& \leq I(M_1; \mathbf{Y}_2^N) + I(M_2; \mathbf{Y}_3^N) + I(M_3; \mathbf{Y}_3^N) \\
& \leq I(M_1, M_3; \mathbf{Y}_2^N, \mathbf{Y}_3^N) + I(M_2; \mathbf{Y}_3^N) \\
& \stackrel{(a)}{=} I(M_1'; \mathbf{Y}_2^N, \mathbf{Y}_3^N) + I(M_2; \mathbf{Y}_3^N) \\
& \stackrel{(b)}{\leq} NI(X_1; Y_2, Y_3 | X_2) + NI(X_2; Y_3), \tag{92}
\end{aligned}$$

where we use M_1' to denote (M_1, M_3) and thus (a) holds; (b) follows by treating M_1' as M_1 in (16).

We deal with those inequalities having U or V in the rest of the proof. The cut-set bound on R_1 is $R_1 \leq I(X_1; Y_2 | X_2)$, but this must be loose because some portion of X_1 carrying the D2D message m_3 is independent of m_1 . (We do not have this issue in the non-D2D scenario.) Therefore, we introduce an auxiliary variable U_n to represent the part of X_1 “related” to R_1 , as follows:

$$U_n = (M_1, M_2, \mathbf{Y}_2^{n-1}, \mathbf{Y}_3^{n-1}), \quad n \in [1 : N], \tag{93}$$

where M_2 , \mathbf{Y}_2^{n-1} , and \mathbf{Y}_3^{n-1} are due to the cut-set bounds on R_1 and R_3 . Note that M_3 is excluded from U_n . Another auxiliary variable V_n is similarly motivated:

$$V_n = (M_2, M_3, \mathbf{Y}_2^{n-1}, \mathbf{Y}_3^{n-1}), \quad n \in [1 : N]. \tag{94}$$

We then apply U and V to improve the cut-set bound. First, consider the bound on R_1 with U_n :

$$\begin{aligned}
N(R_1 - \epsilon_N) & \leq I(M_1; \mathbf{Y}_2^N, \mathbf{X}_2^N) \\
& \leq I(M_1; \mathbf{Y}_2^N, \mathbf{X}_2^N | M_2) \\
& \stackrel{(c)}{=} I(M_1; \mathbf{Y}_2^N | M_2) \\
& = \sum_{n=1}^N I(M_1; Y_{2n} | M_2, \mathbf{Y}_2^{n-1}) \\
& \stackrel{(d)}{=} \sum_{n=1}^N I(M_1; Y_{2n} | M_2, \mathbf{Y}_2^{n-1}, X_{2n}) \\
& \leq \sum_{n=1}^N I(M_1, M_2, \mathbf{Y}_2^{n-1}, \mathbf{Y}_3^{n-1}; Y_{2n} | X_{2n}) \\
& = \sum_{n=1}^N I(U_n; Y_{2n} | X_{2n}) \\
& \leq NI(U; Y_2 | X_2), \tag{95}
\end{aligned}$$

where both of (c) and (d) follow since X_{2n} is a function of (M_2, \mathbf{Y}^{n-1}) . We then use V_n to give another bound on R_1 :

$$\begin{aligned}
N(R_1 - \epsilon_N) & \leq I(M_1; \mathbf{Y}_2^N, \mathbf{X}_2^N) \\
& \leq I(M_1; \mathbf{Y}_2^N, \mathbf{X}_2^N | M_2, M_3) \\
& \stackrel{(e)}{=} I(M_1; \mathbf{Y}_2^N, \mathbf{Y}_3^N | M_2, M_3) \\
& = \sum_{n=1}^N I(M_1; Y_{2n}, Y_{3n} | M_2, M_3, \mathbf{Y}_2^{n-1}, \mathbf{Y}_3^{n-1}) \\
& \stackrel{(f)}{=} \sum_{n=1}^N I(X_{1n}; Y_{2n}, Y_{3n} | M_2, M_3, \mathbf{Y}_2^{n-1}, \mathbf{Y}_3^{n-1})
\end{aligned}$$

$$\begin{aligned}
& \stackrel{(g)}{=} \sum_{n=1}^N I(X_{1n}; Y_{2n}, Y_{3n} | X_{2n}, V_n) \\
& \leq NI(X_1; Y_2, Y_3 | X_2, V), \tag{96}
\end{aligned}$$

where (e) and (g) follow since X_{2n} is a function of $(M_2, \mathbf{Y}_2^{n-1})$, (f) is due to the facts that X_{1n} is a function of (M_1, M_3) and that $M_1 \rightarrow X_{1n} \rightarrow (Y_{2n}, Y_{3n})$ form a Markov chain conditioned on $(M_2, M_3, \mathbf{Y}_2^{n-1}, \mathbf{Y}_3^{n-1})$.

Further, by using U_n , we establish an outer bound on R_3 :

$$\begin{aligned}
N(R_3 - \epsilon_N) & \leq I(M_3; \mathbf{Y}_3^N) \\
& \leq I(M_3; \mathbf{Y}_2^N, \mathbf{Y}_3^N | M_1, M_2) \\
& = \sum_{n=1}^N I(M_3; Y_{2n}, Y_{3n} | M_1, M_2, \mathbf{Y}_2^{n-1}, \mathbf{Y}_3^{n-1}) \\
& \stackrel{(h)}{=} \sum_{n=1}^N I(X_{1n}; Y_{2n}, Y_{3n} | M_1, M_2, \mathbf{Y}_2^{n-1}, \mathbf{Y}_3^{n-1}) \\
& = \sum_{n=1}^N I(X_{1n}; Y_{2n}, Y_{3n} | U_n, X_{2n}) \\
& \leq NI(X_1; Y_2, Y_3 | U, X_2), \tag{97}
\end{aligned}$$

where (h) follows by the same reason as for step (f) in (96). Finally, the auxiliary variable V_n gives rise to the following outer bound on R_3 :

$$\begin{aligned}
N(R_3 - \epsilon_N) & \leq I(M_3; \mathbf{Y}_3^N) \\
& \leq I(M_3; \mathbf{Y}_2^N, \mathbf{Y}_3^N | M_2) \\
& = \sum_{n=1}^N I(M_3; Y_{2n}, Y_{3n} | M_2, \mathbf{Y}_2^{n-1}, \mathbf{Y}_3^{n-1}) \\
& = \sum_{n=1}^N I(M_3; Y_{2n}, Y_{3n} | M_2, \mathbf{Y}_2^{n-1}, \mathbf{Y}_3^{n-1}, X_{2n}) \\
& \leq \sum_{n=1}^N I(M_2, M_3, \mathbf{Y}_2^{n-1}, \mathbf{Y}_3^{n-1}; Y_{2n}, Y_{3n} | X_{2n}) \\
& = \sum_{n=1}^N I(V_n; Y_{2n}, Y_{3n} | X_{2n}) \\
& \leq NI(V; Y_2, Y_3 | X_2). \tag{98}
\end{aligned}$$

Summarizing the above results establishes the outer bound of this theorem.

APPENDIX B PROOF OF PROPOSITION 8

We first introduce a useful lemma:

Lemma 4: Letting

$$Y' = \frac{g_{21}Y_2 + g_{31}Y_3}{\sqrt{|g_{21}|^2 + |g_{31}|^2}}, \tag{99}$$

we have $I(X_1; Y_2, Y_3 | U, X_2) = I(X_1; Y' | U, X_2)$.

Proof: Observe that

$$\begin{aligned}
I(X_1; Y_2, Y_3 | U, X_2) & = I(X_1, Y_2, Y' | U, X_2) \\
& = I(X_1; Y' | U, X_2) + I(X_1; Y_2 | U, X_2, Y'). \tag{100}
\end{aligned}$$

Also, with notation

$$Z'_2 = \frac{|g_{31}|^2 Z_2 - g_{21} g_{31} Z_3}{|g_{21}|^2 + |g_{31}|^2}, \quad (101)$$

we show that

$$\begin{aligned} I(X_1; Y_2 | U, X_2, Y') &\stackrel{(a)}{\leq} I(X_1; Y_2 | X_2, Y') \\ &= I(X_1; Z'_2 | X_2, Y') \\ &\stackrel{(b)}{=} 0, \end{aligned} \quad (102)$$

where (a) follows since $U \rightarrow X_1 \rightarrow Y_2$ form a Markov chain conditioned on (X_2, Y') , (b) follows since Z'_2 is independent of any of (X_1, X_2, Y') . By the squeeze theorem, we must have $I(X_1; Y_2 | U, X_2, Y') = 0$. Substituting this result back in (100) verifies the lemma. ■

Equipped with the above lemma, we continue to prove Proposition 8. We focus on the inequalities (62a) and (62c) which involve the use of auxiliary variables U and V from Theorem 6. Again, use $\rho \in [-1, 1]$ to denote the correlation coefficient $\frac{1}{\sqrt{P_1 P_2}} \mathbb{E}(X_1 X_2)$. It can be shown that

$$\begin{aligned} \log 2\pi e \sigma^2 &\leq h(Y' | U, X_1, X_2) \\ &\leq h(Y' | U, X_2) \\ &\leq h(Y' | X_2) \\ &= \log 2\pi e (\sigma^2 + (1 - \rho^2)(|g_{21}|^2 + |g_{31}|^2)P_1), \end{aligned} \quad (103)$$

so there must exist a constant $\alpha \in [0, 1]$ such that

$$h(Y' | U, X_2) = \log 2\pi e (\sigma^2 + \alpha(1 - \rho^2)(|g_{21}|^2 + |g_{31}|^2)P_1). \quad (104)$$

The outer bound (61d) of Theorem 2 can be evaluated as

$$\begin{aligned} R_3 &\leq I(X_1; Y_2, Y_3 | U, X_2) \\ &\stackrel{(c)}{=} I(X_1; Y' | U, X_2) \\ &= h(Y' | U, X_2) - h(Y' | U, X_1, X_2) \\ &= h(Y' | U, X_2) - h\left(\frac{g_{21} Z_2 + g_{31} Z_3}{\sqrt{|g_{21}|^2 + |g_{31}|^2}}\right) \\ &\stackrel{(d)}{=} \mathcal{C}\left(\frac{\alpha(1 - \rho^2)(|g_{21}|^2 + |g_{31}|^2)P_1}{\sigma^2}\right), \end{aligned} \quad (105)$$

where (c) follows by Lemma 4 and (d) follows by (104).

Moreover, we derive that

$$\begin{aligned} h(Y_2 | U, X_2) &= h(\omega Y' + Z'_2 | U, X_2) \\ &\stackrel{(e)}{\geq} \log \left(2^{h(\omega Y' | U, X_2)} + 2^{h(Z'_2 | U, X_2)} \right) \\ &= \log \left(1 + \alpha(1 - \rho^2)|g_{21}|^2 P_1 \right), \end{aligned} \quad (106)$$

where $\omega = \frac{g_{21}}{\sqrt{|g_{21}|^2 + |g_{31}|^2}}$ and Z'_2 is previously defined in (101); step (e) follows by the entropy power inequality (EPI)

since $\omega Y' \perp\!\!\!\perp Z'_2$ given (U, X_2) . Consequently, we have

$$\begin{aligned} R_1 &\leq I(U; Y_2 | X_2) \\ &= h(Y_2 | X_2) - h(Y_2 | U, X_2) \\ &\stackrel{(f)}{\leq} \mathcal{C}\left(\frac{(1 - \rho^2)|g_{21}|^2 P_1}{\sigma^2 + \alpha(1 - \rho^2)|g_{21}|^2 P_1}\right), \end{aligned} \quad (107)$$

where (f) is due to (106).

Next, we show the upper bounds on R_1 or R_3 that involve the auxiliary variable V . First, we derive the following chain of inequalities:

$$\begin{aligned} I(X_1; Y_2, Y_3 | V, X_2) &\stackrel{(g)}{\leq} I(X_1; Y_2, Y_3 | X_2) \\ &= \mathcal{C}\left(\frac{(1 - \rho^2)(|g_{21}|^2 + |g_{31}|^2)P_1}{\sigma^2}\right), \end{aligned} \quad (108)$$

where (g) follows since $V \rightarrow X_1 \rightarrow (Y_2, Y_3)$ form a Markov chain conditioned on X_2 . Thus, we are guaranteed to find a constant $\beta \in [0, 1]$ such that

$$\begin{aligned} R_1 &\leq I(X_1; Y_2, Y_3 | V, X_2) \\ &= \mathcal{C}\left(\frac{\beta(1 - \rho^2)(|g_{21}|^2 + |g_{31}|^2)P_1}{\sigma^2}\right). \end{aligned} \quad (109)$$

Finally, we can compute (61e) as

$$\begin{aligned} R_3 &\leq I(V; Y_2, Y_3 | X_2) \\ &= I(X_1; Y_2, Y_3 | X_2) - I(X_1; Y_2, Y_3 | V, X_2) \\ &\stackrel{(h)}{=} I(X_1; Y_2, Y_3 | X_2) - \mathcal{C}\left(\frac{\beta(1 - \rho^2)(|g_{21}|^2 + |g_{31}|^2)P_1}{\sigma^2}\right) \\ &\leq \mathcal{C}\left(\frac{(1 - \rho^2)(|g_{21}|^2 + |g_{31}|^2)P_1}{\sigma^2 + \beta(1 - \rho^2)(|g_{21}|^2 + |g_{31}|^2)P_1}\right), \end{aligned} \quad (110)$$

where (h) is due to the identity in (109). We have established the set of inequalities (62a) and (62c). The verification of the remaining inequalities in (62) is similar to the proof of Proposition 3.

REFERENCES

- [1] J. I. Choi, M. Jain, K. Srinivasan, P. Levis, and S. Katti, "Achieving single channel, full duplex wireless communication," in *ACM Int. Conf. Mobile Comput. Netw. (MobiCom)*, Aug. 2010, pp. 375–386.
- [2] E. Aryafar, M. Khojastepour, K. Sundaresan, S. Rangarajan, and M. Chiang, "MIDU: Enabling MIMO full duplex," in *ACM Int. Conf. Mobile Comput. Netw. (MobiCom)*, 2012, pp. 257–268.
- [3] E. Everett, A. Sahai, and A. Sabharwal, "Passive self-interference suppression for full-duplex infrastructure nodes," *IEEE Trans. Wireless Commun.*, vol. 13, no. 2, pp. 680–694, Feb. 2014.
- [4] A. Sabharwal, P. Schniter, D. Guo, D. W. Bliss, S. Rangarajan, and R. Wichman, "In-band full-duplex wireless: Challenges and opportunities," *IEEE J. Sel. Areas Commun.*, vol. 32, no. 9, pp. 1637–1652, Sept. 2014.
- [5] X. Xie and X. Zhang, "Does full-duplex double the capacity of wireless networks?," in *IEEE INFOCOM*, Apr. 2014, pp. 253–261.
- [6] S. Goyal, P. Liu, S. S. Panwar, R. A. Difazio, R. Yang, and E. Bala, "Full duplex cellular systems: will doubling interference prevent doubling capacity?," *IEEE Commun. Mag.*, vol. 53, no. 5, pp. 121–127, May 2015.
- [7] K. Marton, "A coding theorem for the discrete memoryless broadcast channel," *IEEE Trans. Inf. Theory*, vol. 25, no. 3, pp. 306–311, May 1979.
- [8] R. Tannious and A. Nosratinia, "Relay channel with private messages," *IEEE Trans. Inf. Theory*, vol. 53, no. 10, pp. 3777–3785, Oct. 2007.

- [9] Y. Liang and V. V. Veeravalli, "Cooperative relay broadcast channels," *IEEE Trans. Inf. Theory*, vol. 53, no. 3, pp. 900–928, Mar. 2007.
- [10] Y. Liang and G. Kramer, "Rate regions for relay broadcast channels," *IEEE Trans. Inf. Theory*, vol. 53, no. 10, pp. 3517–3535, Oct. 2007.
- [11] S. Goyal, P. Liu, S. Panwar, R. A. DiFazio, R. Yang, J. Li, and E. Bala, "Improving small cell capacity with common-carrier full duplex radios," in *IEEE Int. Conf. Commun. (ICC)*, June 2014.
- [12] C. Karakus and S. Diggavi, "Opportunistic scheduling for full-duplex uplink-downlink networks," in *IEEE Int. Symp. Inf. Theory (ISIT)*, June 2015, pp. 1019–1023.
- [13] S. Shao, D. Liu, K. Deng, Z. Pan, and Y. Tang, "Analysis of carrier utilization in full-duplex cellular networks by dividing the co-channel interference region," *IEEE Commun. Lett.*, vol. 18, no. 6, pp. 1043–1046, June 2014.
- [14] J.-H. Yun, "Intra and inter-cell resource management in full-duplex heterogeneous cellular networks," *IEEE Trans. Mobile Comput.*, vol. 15, no. 2, pp. 392–405, Feb. 2016.
- [15] J. Marašević, J. Zhou, H. Krishnaswamy, Y. Zhong, and G. Zussman, "Resource allocation and rate gains in practical full-duplex systems," *IEEE/ACM Trans. Netw.*, vol. 25, no. 1, pp. 292–305, Feb. 2017.
- [16] K. Shen and W. Yu, "Interference management in full-duplex wireless cellular networks via fractional programming," in *IEEE Veh. Technol. Conf. (VTC) Spring*, June 2018.
- [17] S. H. Chae, S. H. Lim, and S.-W. Jeon, "Degrees of freedom of full-duplex multi-antenna cellular networks," *IEEE Trans. Wireless Commun.*, vol. 17, no. 2, pp. 982–995, Feb. 2018.
- [18] S. H. Chae, S.-W. Jeon, and S. H. Lim, "Fundamental limits of spectrum sharing full-duplex multicell networks," *IEEE J. Sel. Areas Commun.*, vol. 34, no. 11, pp. 3048–3061, Nov. 2016.
- [19] M. A. Khojastepour, K. Sundaresan, and S. Rangarajan, "Scaling wireless full-duplex in multi-cell networks," in *IEEE INFOCOM*, May 2015, pp. 1751–1759.
- [20] P. Razaghi and W. Yu, "Bilayer low-density parity-check codes for decode-and-forward in relay channels," *IEEE Trans. Inf. Theory*, vol. 53, no. 10, pp. 3723–3739, Oct. 2007.
- [21] R. H. Etkin, D. N. C. Tse, and H. Wang, "Gaussian interference channel capacity to within one bit," *IEEE Trans. Inf. Theory*, vol. 54, no. 12, pp. 5534–5562, Nov. 2008.
- [22] B. Wang, J. Zhang, and A. Høst-Madsen, "On the capacity of MIMO relay channels," *IEEE Trans. Inf. Theory*, vol. 51, no. 1, pp. 29–43, Jan. 2005.
- [23] H. Sato, "An outer bound to the capacity region of broadcast channels," *IEEE Trans. Inf. Theory*, vol. 24, no. 3, pp. 374–377, May 1978.
- [24] R. S. Cheng and S. Verdú, "Gaussian multiaccess channels with ISI: Capacity region and multiuser water-filling," *IEEE Trans. Inf. Theory*, vol. 39, no. 3, pp. 773–785, May 1993.